Supporting Information

Adaptive coordination assemblies based on a flexible tetraazacyclododecane ligand for promoting carbon dioxide fixation

Shaochuan Li,[ab] Caiping Liu,[a] Qihui Chen*,[a] Feilong Jiang,[a] Daqiang Yuan,[a] Qing-fu Sun*,[a] and Maochun Hong*[a]

[a] State Key Laboratory of Structure Chemistry, Fujian Institute of Research on the Structure of Matter, Chinese Academy of Sciences, Fuzhou, Fujian, 350002 (China)

[b] University of the Chinese Academy of Sciences, Beijing, 100049 (China).

Table of Contents

1. **Materials**
2. **Methods**
3. **Single crystal X-ray diffraction studies**
4. **Computational methods**
5. **Supplementary Figures and Tables**
6. **References**

Experimental Procedures

Materials

Unless otherwise stated, all chemicals and solvents were purchased from commercial companies and used without further purification. 1D and 2D-NMR spectra were measured on a Bruker Biospin Avance III (400 MHz) spectrometer or JEOL JNM-ECZ400S/L1 NMR (400 MHz) spectrometer. The1,4,7,10-tetrazaz-cyclododecane-N,N',N'',N'''-tetra-p-methylpyridine and Me_4en-$Pd(NO_3)_2$ were synthesized according to the literatures [1-3].

Methods

Synthesis of the Ligand L

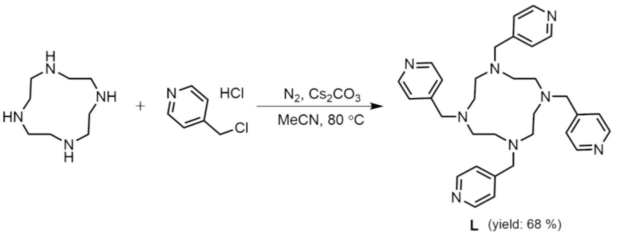

Scheme S 1 The synthesis of **L**.

Under dinitrogen, cyclen (0.688 g, 4.0 mmol) was dissolved in 140 mL of MeCN and 20 mol equiv. of Cs_2CO_3 (26.0 g, 80.0 mmol) was added as a solid to form a suspension. A total of 4.1 mol equiv. of 4-(Chloromethyl)pyridine Hydrochloride (2.69 g, 16.4 mmol) in 10 mL MeCN was then added dropwise to the cyclen solution. The reaction mixture was subsequently heated to reflux temperature (80 °C) under nitrogen for 24 h, after which the solution was filtered to remove the inorganic salts, and all volatiles were removed under reduced pressure. The crude material was purified by silica gel flash column (v/v, CH_2Cl_2:PE = 2:1) to give ligand **L** as pale-yellow powder (1.45g, 2.72 mmol, 68.0% yield). ^{1}H NMR (400 MHz, 298 K, DMSO-d_6) δ 8.38 (s, 8H), 7.38 (s, 8H), 3.45 (s, 8H), 2.65 (s, 16H). ^{13}C NMR (101 MHz, 298 K, DMSO-d_6) δ 150.40 (s), 140.19 (s), 127.32 (s), 54.26 (s), 47.82 (s).

The crystal structure of **L** was obtained through slow evaporation of the 3.5 mL CH_3CN solution of ligand (7.13 mg, 0.013 mmol) and $Eu(CF_3SO_3)_3$ (9.55 mg, 0.0156 mmol).

Synthesis of the ZnL Ligand

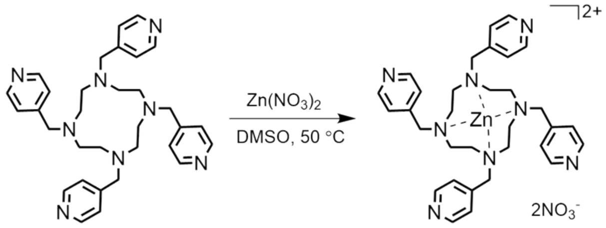

Scheme S 2 The synthesis of **ZnL**.

The ligand 1,4,7,10-tetrazaz-cyclododecane-N,N',N'',N'''-tetra-p-methylpyridine (**L**) (55.28 mg, 0.103 mmol) and $Zn(NO_3)_2(H_2O)_6$ (30.64 mg, 0.103 mmol) were added into a 5 mL glass vial with 4 mL DMSO, further stirring this mixture at 50 °C for 3 hours led to a homogeneous pale yellow solution. ^{1}HNMR confirms the quantitative formation of the ligand **ZnL(NO_3)$_2$**. ^{1}H NMR (400 MHz, 298 K, DMSO-*d$_6$*) δ 8.73 (d, *J* = 5.7 Hz), 7.74 (d, *J* = 5.9 Hz), 4.46 (s), 3.05 (d, *J* = 4.4 Hz), 2.79 (d, *J* = 7.3 Hz). ^{13}C NMR (101 MHz, 298 K, DMSO-*d$_6$*) δ 150.40 (s), 140.19 (s), 127.32 (s), 99.95 (s), 54.29 (s), 47.95 (s).

Suitable crystals of **ZnL** for X-ray diffraction could be obtained by slow evaporation of the CH_3CN solution of **ZnL**.

Typical procedure for the synthesis of Zn-chelated coordination tubes [(PdMe$_4$en)$_6$(ZnL)$_3$]$^{18+}$ based on ZnL ligand

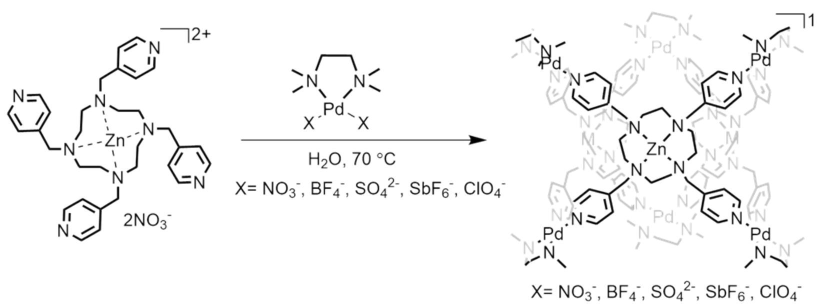

Scheme S 3 Synthesis of Zn-chelated coordination tubes **[(PdMe$_4$en)$_6$(ZnL)$_3$]$^{18+}$** (**1-Zn**) based on **ZnL** ligand.

Adding the new-formed **ZnL** ligand (19.46 mg, 0.0268 mmol) and $Me_4enPd(NO_3)_2$ (18.58 mg, 0.0536 mmol) into a 5 mL glass vial with 2.5 mL D_2O, then stirring this mixture at 70 °C for 3 hours quantitatively led to the coordination tube **1-Zn**. ^{1}H NMR (400 MHz, 298 K, D_2O): δ 9.10 (d, *J* = 4.5 Hz, 12H), 9.02 (d, *J* = 6.4 Hz, 12H), 7.77 (d, *J* = 4.7 Hz, 12H), 7.69 (d, *J* = 5.8 Hz, 12H), 4.33 (d, *J* = 14.7 Hz, d, *J* = 4.5 Hz, 12H), 4.19 (d, *J* = 13.0 Hz, d, J = 4.5 Hz, 12H), 3.02 (s, 24H), 2.67 (d, *J* = 16.5 Hz, 72H), 2.96 (d, *J* = 43.9 Hz, 12H), 1.88 (m, 12H). ^{13}C NMR (101 MHz, 298 K, D_2O): δ 151.59 (d, J = 11.5 Hz), δ 150.18 (m), δ 143.59 (m), δ 131.21(m), δ 129.21 (m), δ 62.57 (s), δ 53.41 (m), δ 50.18 (s), δ 47.96 (m).

Colorless single crystals of **1-Zn**(NO_3^-) suitable for X-ray diffraction could be obtained by slowly diffusing the THF vapor into the aqueous solution of **1-Zn**(NO_3^-).

Typical procedure for the one pot synthesis of Zn-chelated coordination tubes 1-Zn.

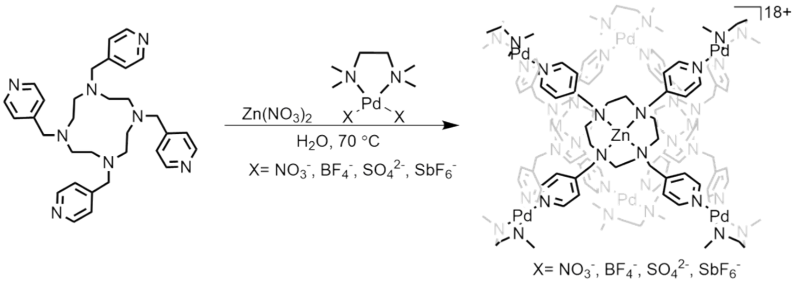

Scheme S 4 One pot synthesis of Zn-chelated coordination tubes **$[(PdMe_4en)_6(ZnL)_3]^{18+}$** (**1-Zn**).

The ligand 1,4,7,10-tetrazaz-cyclododecane-N,N',N'',N'''-tetra-p-methylpyridine (**L**) (18.25 mg, 0.034 mmol), $Zn(NO_3)_2(H_2O)_6$ (10.12 mg, 0.034 mmol) and $Me_4enPd(NO_3)_2$ (23.57 mg, 0.068 mmol) were added to 5 mL glass vial with 2.0 mL D_2O, further stirring this mixture at 70 °C for 3 hours could quantitatively lead to coordination tube **1-Zn**.

Typical procedure for the synthesis of chelated Co(II)/Ni(II)/Cu(II) coordination tubes

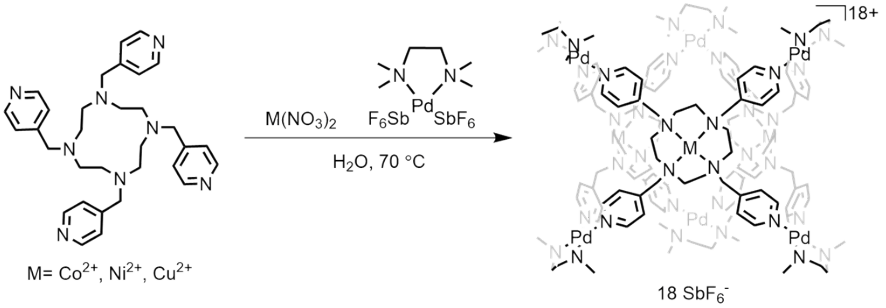

Scheme S 5 Synthesis of chelated Co(II)/Ni(II)/Cu(II) coordination tubes.

The ligand 1,4,7,10-tetrazaz-cyclododecane-N,N',N'',N'''-tetra-p-methylpyridine (**L**) (23.08 mg, 0.043 mmol), $Co(NO_3)_2(H_2O)_6$ (12.52 mg, 0.043 mmol) and $Me_4enPd(SbF_6)_2$ (59.68 mg, 0.086 mmol) were added to 5 mL glass vial with 2.5 mL D_2O, further stirring this mixture at 70 °C for 3 hours could quantitatively lead to coordination tube **1-Co**. ^1H NMR (400 MHz, 298 K, D_2O) δ 9.05 (d, *J* = 5.6 Hz, 12H), 8.99 (d, *J* = 5.9 Hz, 12H), 7.69 (d, *J* = 3.6 Hz, 12H), 7.65 (d, *J* = 5.9 Hz, 12H), 4.34 (d, *J* = 14.8 Hz, 12H), 4.23 (d, *J* = 13.6 Hz, 12H), 2.98 (s, 24H), 2.91 (s, 18H), 2.53 (d, *J* = 17.9 Hz, 72H), 2.43 – 1.97 (m, 30H). ^{13}C NMR (101 MHz, 298 K, D_2O): δ 151.41 (s), 150.93 (s), 131.05 (s), 129.25 (m), 62.49 (s), 53.28 (s), 50.14(d, *J* = 26.8 Hz), 47.79 (m).

Coordination tube **1-Ni** and **1-Cu** were synthesized as the same method above.

Purple single crystals of **1-Co** suitable for X-ray diffraction could be obtained by slowly diffusing THF vapor into the NO_3^- aqueous solution of **1-Co**.

Green single crystals of **1-Ni** suitable for X-ray diffraction could be obtained by adding an appropriate amount of SO_4^{2-} into the NO_3^- aqueous solution of **1-Ni** and then diffusing THF vapor to the new-fromed mixed solution.

Blue single crystals of **1-Cu** suitable for X-ray diffraction could be obtained by slowly diffusing THF vapor into the NO_3^- aqueous solution of **1-Cu**.

Typical procedure for the synthesis of Ag-chelated coordination cages 2.

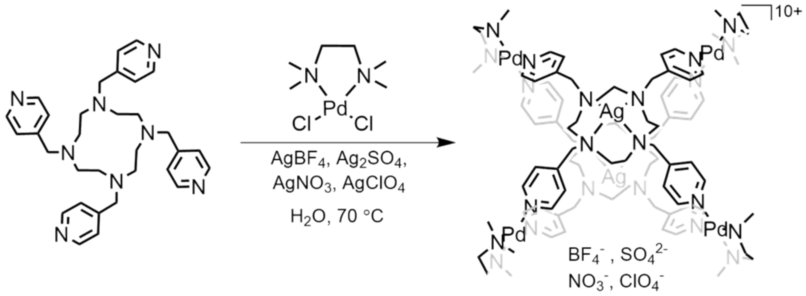

Scheme S 6 Synthesis of Ag-chelated coordination cages **[(PdMe$_4$en)$_4$(AgL)$_2$]$^{12+}$** (**2**).

The ligand 1,4,7,10-tetrazaz-cyclododecane-N,N',N'',N'''-tetra-p-methylpyridine (**L**) (7.30 mg, 0.0136 mmol) and Me$_4$enPdCl$_2$ (7.97 mg, 0.0272 mmol), AgBF$_4$ (13.25 mg, 0.068 mmol) were added to 5 mL glass vial with 1.5 mL D$_2$O, further stirring this mixture at 70 °C for 3 hours after which the solution was filtered to remove the precipitation AgCl, led to a homogeneous yellow solution of coordinantion cage **2**(BF$_4^-$).^{1}HNMR confirms the quantitative formation of coordination cage **2**(BF$_4^-$). ^{1}H NMR (400 MHz, 298 K, D$_2$O): δ 9.01 (d, *J* = 5.9 Hz, 8H), 8.87 (d, *J* = 5.8 Hz, 8H), 7.59 (d, *J* = 5.9 Hz, 8H), 7.31 (d, *J* = 7.3 Hz, 8H), 4.28 (d, *J* = 14.3 Hz, 8H), 4.02 (d, *J* = 14.4 Hz, 8H), 3.26 (d, *J* = 12.7 Hz, 8H), 3.14 (s, 16H), 2.78 (s, 48H), 1.51 (dd, *J* = 25.1, 12.8 Hz, 16H), 1.05 (d, *J* = 13.4 Hz, 8H). ^{13}C NMR (101 MHz, 298 K, D$_2$O): δ 150.62 (s), 143.54 (s), 130.19 (s), 129.19 (s), 63.01 (s), 62.65 (s), 55.17 (s), 50.21 (d, *J* = 12.8 Hz), 43.32 (s).

The coordination cage **2**(SO$_4^{2-}$, NO$_3^-$, ClO$_4^-$, SbF$_6^-$) was synthesized with the same method as above.

Pale yellow single crystals of **2**(BF$_4^-$)/**2**(SO$_4^{2-}$) suitable for X-ray diffraction could be obtained by slowly diffusing THF vapor into the aqueous solution of **2**(BF$_4^-$)/**2**(SO$_4^{2-}$).

Typical procedure for the synthesis of Pd-chelated coordination tubes [(PdMe$_4$en)$_6$(PdL)$_3$]$^{18+}$ (3)

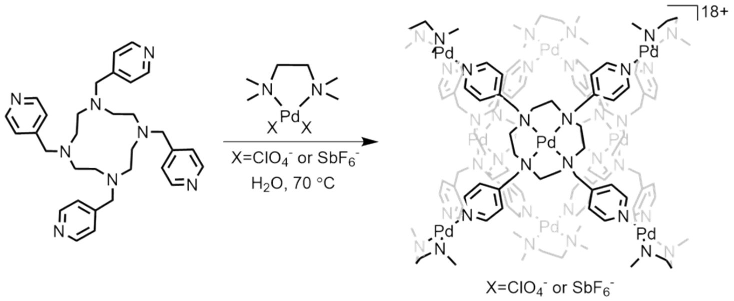

Scheme S 7 Synthesis of Pd-chelated coordination tubes **[(PdMe$_4$en)$_6$(PdL)$_3$]$^{18+}$** (**3**).

The ligand 1,4,7,10-tetrazaz-cyclododecane-N,N',N'',N'''-tetra-p-methylpyridine (**L**) (12.34 mg, 0.023 mmol) and Me$_4$enPd(ClO$_4$)$_2$ (29.10 mg, 0.069 mmol) were added into a 5mL glass vial with 2.5 mL D$_2$O, further stirring this mixsture 70 °C for 3 hours led to a homogeneous yellow solution. ^{1}HNMR confirms the formation of coordination tube **3**(ClO_4^-).^{1}H NMR (400 MHz, 298 K, D_2O): ^{1}HNMR (400 MHz, 298 K, D_2O): δ 9.06 (d, *J* = 3.1 Hz, 12H), 8.99 (d, *J* = 4.8 Hz, 12H), 7.73 (d, *J* = 4.5 Hz, 12H), 7.64 (d, *J* = 2.8 Hz, 12H), 4.30 (d, *J* = 9.7 Hz, 12H), 4.17 (d, *J* = 7.9 Hz, 12H), 3.10 (s, 24H), 2.69 (s, 72H), 2.42 (d, *J* = 33.8 Hz, 36H), 1.96 (s, 12H). ^{13}C NMR (4101 MHz, 298 K, D_2O): δ 151.70 (s), 150.17 (s), 130.85 (s), 129.87 (s), 128.50 (d, *J* = 9.5 Hz), 62.89 (s), 62.56 (d, *J* = 13.3 Hz), 53.67 (m), 50.17 (s), 48.46(d, *J* = 15.8 Hz), 46.59 (s).

The coordination tube **3**(SbF_6^-) was synthesized with the same method as above.

Pale yellow single crystals of **3**(ClO_4^-) suitable for X-ray diffraction could be obtained by slow evaporation of the aqueous solution of **3**(ClO_4^-).

Typical procedure for the transformation from cage 2(BF_4^-) to tube 1-Zn

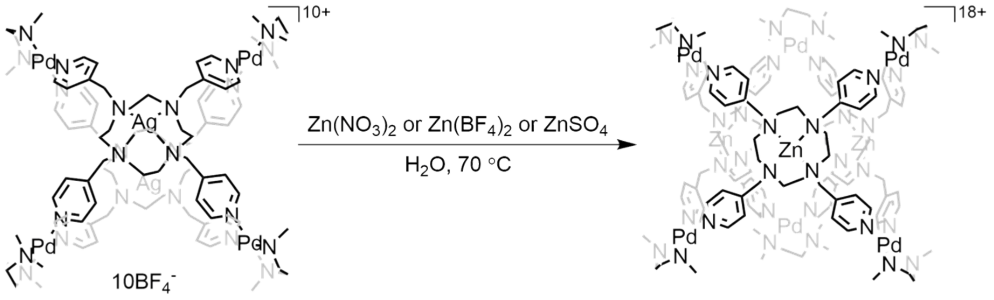

Scheme S 8 Transformation from cage **2** to tube **1-Zn** induced by Zn(II).

Different amounts of $Zn(NO_3)_2(H_2O)_6$ (0.5 M solution, from 1 equiv. to 80 equiv.) were continuously added into a 5 mL glass bottle containing 0.8 mL D_2O of cages **2**(BF_4^-) (4.26 mg, 1.38 μmol) and stirred at 70 °C for 3 hours. Then, ^{1}HNMR was performed to determine whether the conversion was complete.

Typical procedure for the transformation from tube 1-Zn(NO_3^-) to cage 2

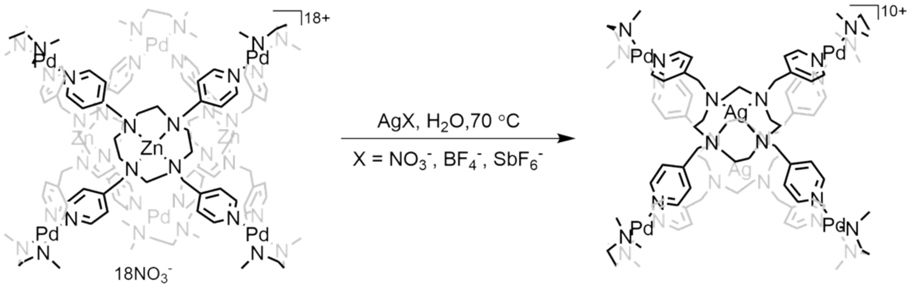

Scheme S 9 Transformation from tube **1-Zn**(NO_3^-) to cage **2** induced by Ag(I).

Different amounts of $AgNO_3$ (2 M solution, from 3 equiv. to 100 equiv.) were continuously added into a 5 mL glass bottle containing 0.7 mL D_2O of tubes **1-Zn**(NO_3^-) (13.20 mg, 3.10 μmol) and stirred at 70 °C for 3 hours. Then, ^{1}HNMR was performed to determine whether the conversion was complete.

Other different anionic Ag$^+$ (BF_4^-,SbF_6^-) metal salts induced transformation from tube **1-Zn**(NO_3^-) to cage **2** as the same method above.

Typical procedure for the transformation from cage 2(BF_4^-) **to tube 3**

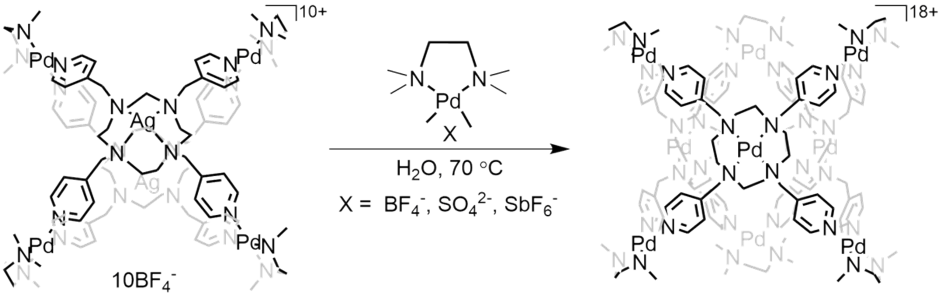

Scheme S 10 Transformation from cage **2**(BF_4^-) to tube **3** induced by Me$_4$en-Pd(II).

Different amounts of Me$_4$en-Pd(BF_4)$_2$ (0.5 M solution, from 3 equiv. to 130 equiv.) were continuously added into a 5 mL glass bottle containing 0.7 mL D_2O of cages **2**(BF_4^-) (6.02 mg, 1.95 μmol) and stirred at 70 °C for 3 hours. Then, ^{1}HNMR was performed to determine whether the conversion was complete.

Other different anionic Me$_4$en-Pd(II) metal links induced transformation from cage **2**(BF_4^-) to tube **3** as the same method above.

Typical procedure for the transformation from tube 3(SbF_6^-) **to cage 2**

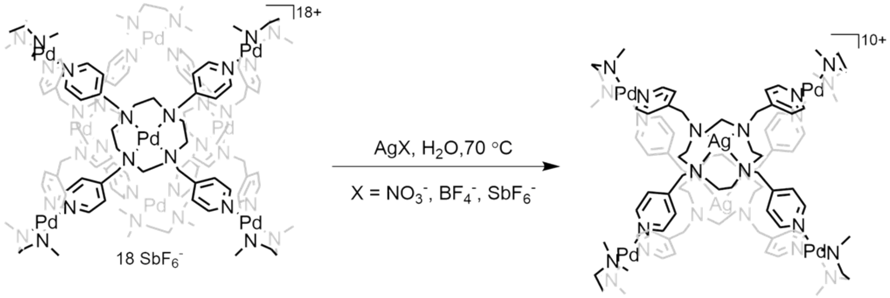

Scheme S 11 Transformation from tube **3**(SbF_6^-) to cage **2** induced by Ag(I).

Different amounts of $AgNO_3$ (2 M solution, from 1 equiv. to 30 equiv.) were continuously added into a 5 mL glass bottle containing 0.7 mL D_2O of tubes **3**(SbF_6^-) (9.40 mg, 1.25 μmol) and stirred at 70 °C for 3 hours. Then, ^{1}HNMR was performed to determine whether the conversion was complete.

Other different anionic Ag$^+$ (BF_4^-, SbF_6^-) metal salts induced transformation from tube **3**(SbF_6^-) to cage **2** as the same method above.

Typical procedure for the acid-base stability test of coordination tubes

Coordination tube **1-Zn**(NO_3^-) **[(PdMe$_4$en)$_6$(ZnL)$_3$(NO$_3$)$_{18}$]** (53.65 mg, 0.0126 mmol) was dissolved in 0.67 mL D_2O solution with different pH values (from pH 0 to pH 13). After 3 hours, ^{1}H NMR was performed to determine whether the tubular structure was destroyed.

Synthesis of the $PdMe_4enPy_2(NO_3)_2$

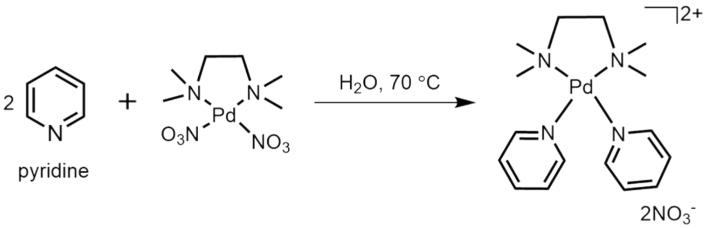

Scheme S 12 Synthesis of **$PdMe_4enPy_2(NO_3)_2$**.

The pyridine (**Py**) (73.88 mg, 0.934 mmol) and $PdMe_4en(NO_3)_2$ (161.88 mg, 0.467 mmol) were added into a 5 mL glass vial with 3 mL D_2O. Further stirring this mixture at 70 °C for 3 hours led to a homogeneous pale yellow solution. ^{1}HNMR confirms the quantitative formation of **$PdMe_4en(Py)_2(NO_3)_2$**. ^{1}H NMR (400 MHz, 298 K, D_2O): δ 8.97 (d, *J* = 5.0 Hz, 4H), 7.95 (t, *J* = 7.8 Hz, 2H), 7.57 (d, *J* = 7.7 Hz, 4H), 3.07 (s, 4H), 2.62 (s, 12H).

Synthesis of $Zn(L^1)(NO_3)_2$

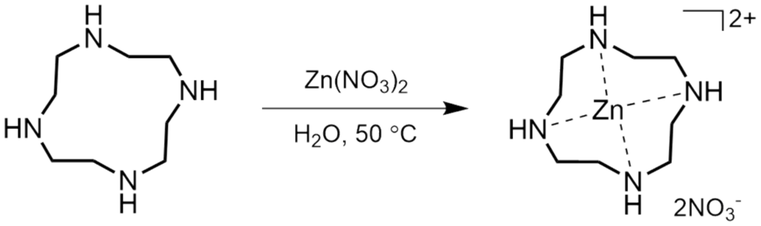

Scheme S 13 Synthesis of **ZnL^1**.

The 1,4,7,10-tetraazacyclododecane (**L^1**) (39.97 mg, 0.232 mmol) and $Zn(NO_3)_2(H_2O)_6$ (69.32 mg, 0.233 mmol) were added into 5 mL glass vial with 4 mL D_2O. Further stirring this solution at 50 °C for 3 hours led to a homogeneous pale colorless solution. ^{1}H NMR confirms the quantitative formation of **ZnL^1**$(NO_3)_2$. ^{1}H NMR (400 MHz, 298 K, D_2O): δ 2.90 (dd, *J* = 12.0, 6.7 Hz, 8H), 2.77 (dd, *J* = 7.9, 2.6 Hz, 8H).

Carbon dioxide fixation experiments

The CO_2 dissolution experiment

2.1 mL of the solution was added into a 20 mL glass tube and CO_2 gas was continuously injected into this solution. After 7 minutes, the content of CO_2 in the solution was measured by the ^{13}C NMR.

Blank experiment

2 mL of D_2O, 1 mL of DMSO-*d6*, and 0.03 mmol NaOH were firstly added into a 20 mL glass tube, then CO_2 gas

was continuously injected into this solution under slowly stirring. After 3 hours, ^{13}C NMR was performed to determine whether there was CO_3^{2-} in the solution.

Typical procedure CO_2 conversion process assisted by tube 1-Zn, ZnL^1, 1-Co, 1-Ni

2 mL of D_2O, 1 mL of DMSO-*d6*, 0.03 mmol NaOH, and 0.015 mmol tube **1-Zn** (63.87 mg) were firstly added into a 20 mL glass tube, then CO_2 gas was continuously injected into this solution under slowly stirring. After 3 hours, ^{13}C NMR was performed to determine whether there was CO_3^{2-} in the solution.

After reaction, adding equivalent of $Ca(NO_3)_2$ into this solution could realize the recycling of tube **1-Zn**.

Other catalysts **ZnL^1, 1-Co** and **1-Ni** carried out the CO_2 conversion process as the same method above.

Single crystal X- ray diffraction studies

The X-ray diffraction data for crystals of **L**, **ZnL**, **1-Zn**, **2**(BF_4^-), **2**(SO_4^{2-}), **3**(ClO_4^-), **1-Co**, **1-Ni**, **1-Cu** and **1-Zn-CO_3^{2-}** were collected on a Bruker D8 Venture diffractometer with Mo Kα radiation. Data reduction was performed with APEX 3 software program and absorption corrections were performed using a multi-scan method. Those crystal data were solved by direct methods and refined by full-matrix least-squares on F^2 with anisotropic displacement using the OLEX-2 software [4]. Solvent molecules were highly disordered, and therefore they could not be reasonably located. These residual intensities were removed by PLATON/SQUEEZE routine [5].

Computational methods

Computational method for cavity volumes

Cavity volumes of tubes **1-Zn**, **3**(ClO_4^-), **1-Co**, **1-Ni**, **1-Cu**, **1-Zn-CO_3^{2-}** were calculated by using 3V webserver. [6] Atom coordinates was adopted from the crystal structure of respective structure. An outer probe radius of 10.0 Å and an inner probe radius of 1.0 Å were used. The cavity volume was estimated as respective values and graphics were generated with UCSF Chimera, [7] where all structures were depicted in stick model and the cavity was shown as purple surface.

Computational method for the binding energy between $[CO_3]^{2-}$ and the tubular cavity of 1-Zn-CO_3^{2-}

The binding energy between $[CO_3]^{2-}$ and cluster skeleton was calculated by using the Density functional theory (DFT) methods. The PBE-type exchange-correlation functional[8] with generalized gradient approximation (GGA) and the Double Numerical plus polarization (DND) basis sets[9] that include a d-type polarization function on all non-hydrogen atoms were employed for all calculations. In addition, the Grimme DFT-D correction method[10] was selected to describe the weak hydrogen bonding interaction, and the DFT Semi-core Pseudopots (DSPP) method[11] was used simultaneously to reduce the computational cost. For all calculations, the FINE quality mesh size and the strict convergence limits were employed. For the cluster-$[CO_3]^{2-}$ system, the coordinates were chosen from the its crystal data. Whereas for the hypothetical cluster-$[NO_3]^-$ system, the cluster skeleton was fixed and only the $[NO_3]^-$ anion was optimized based on the above method. All of these calculations were performed by using the Dmol^3 module integrated in the Material Studio program package.[12] The binding energy between anion and cluster was calculated in terms of the equation

$\Delta E_b = E_{cluster\text{-}anion} - E_{cluster} - E_{anion}$

where $E_{cluster\text{-}anion}$, $E_{cluster}$ and E_{anion} stands for the energies of the anion-encased cluster, the bare cluster and the isolated anion, respectively. According to this equation, the more negative binding energy, the easier it is for the anions to be wrapped into the cavity and the more stable the structure.

The calculated results reveal that $[CO_3]^{2-}$ is easy to be wrapped into the cavity and can stabilize the cluster structure, which is consistent with the experimental observation.

Results and Discussion

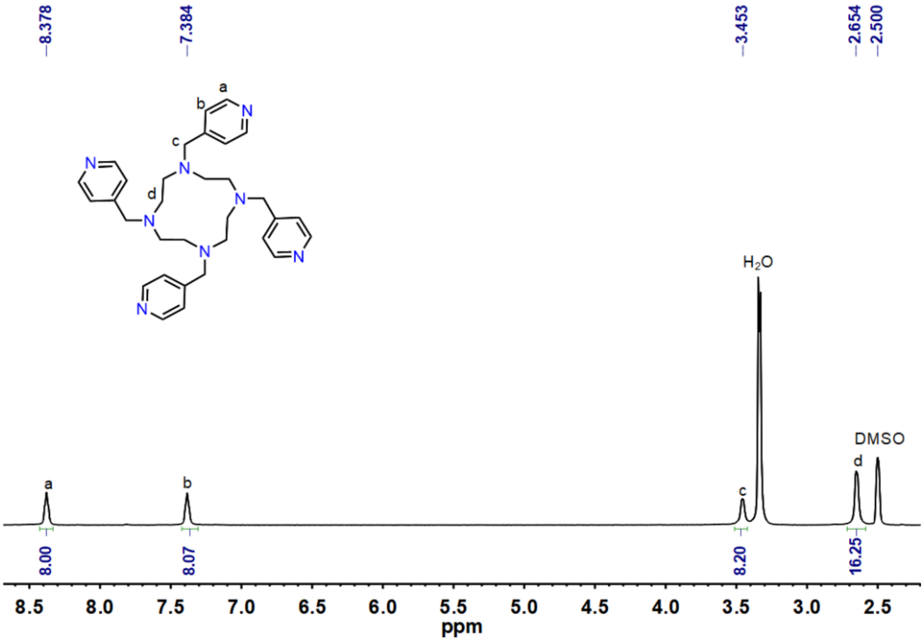

Figure S 1 The ^1H NMR spectrum of **L** (400 MHz, DMSO-$_{d6}$, 298 K).

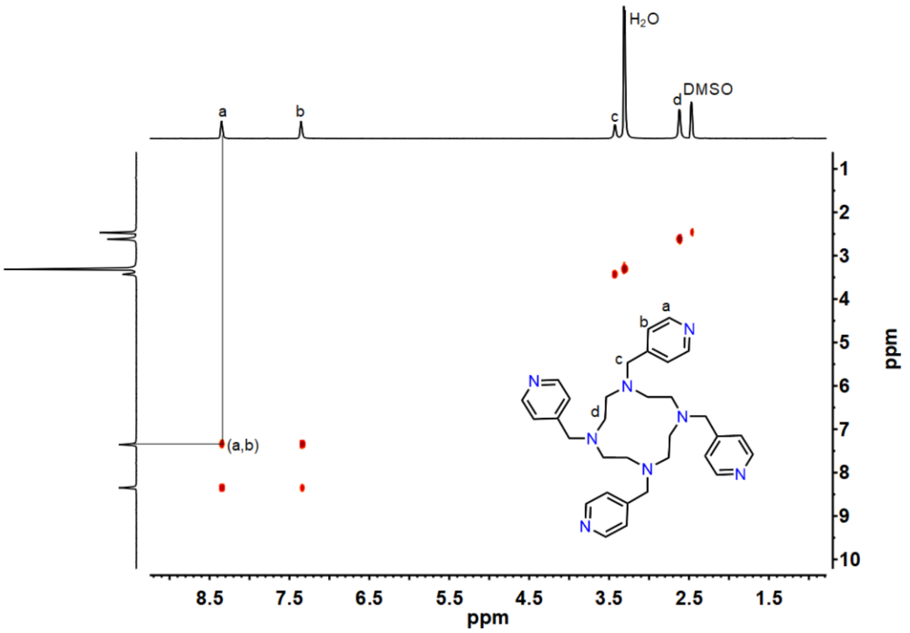

Figure S 2 The ^{1}H-^{1}H COSY spectrum of **L** (400 MHz, DMSO-$_{d6}$, 298 K).

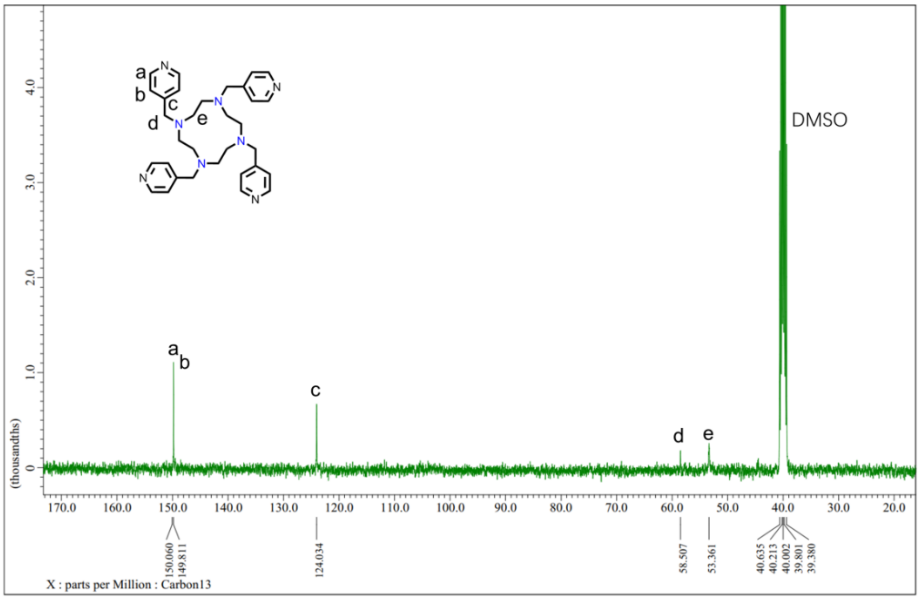

Figure S 3 The ^{13}C NMR spectrum of **L** (101 MHz, DMSO-$_{d6}$, 298 K).

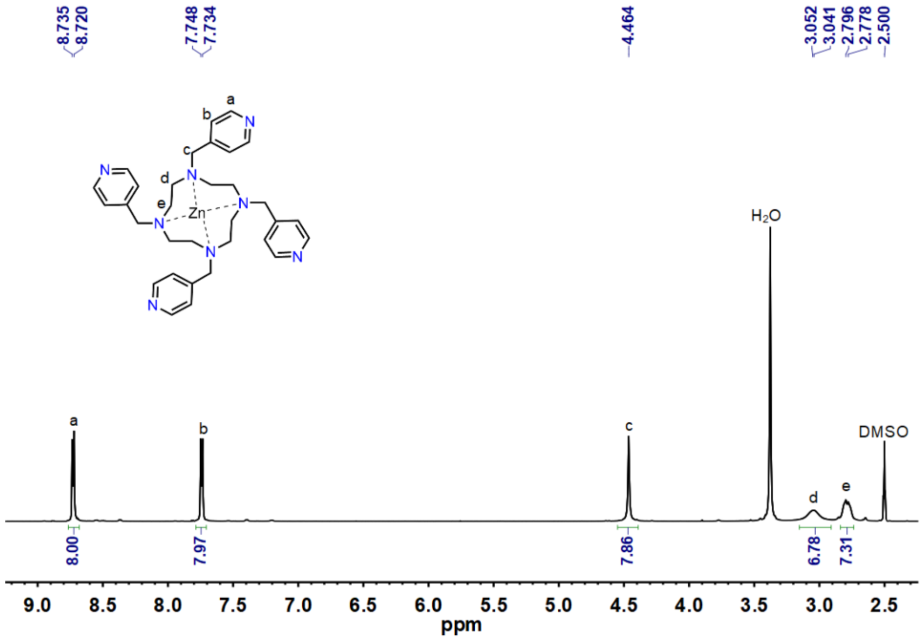

Figure S 4 The ^{1}H NMR spectrum of **ZnL** (400 MHz, DMSO-$_{d6}$, 298 K).

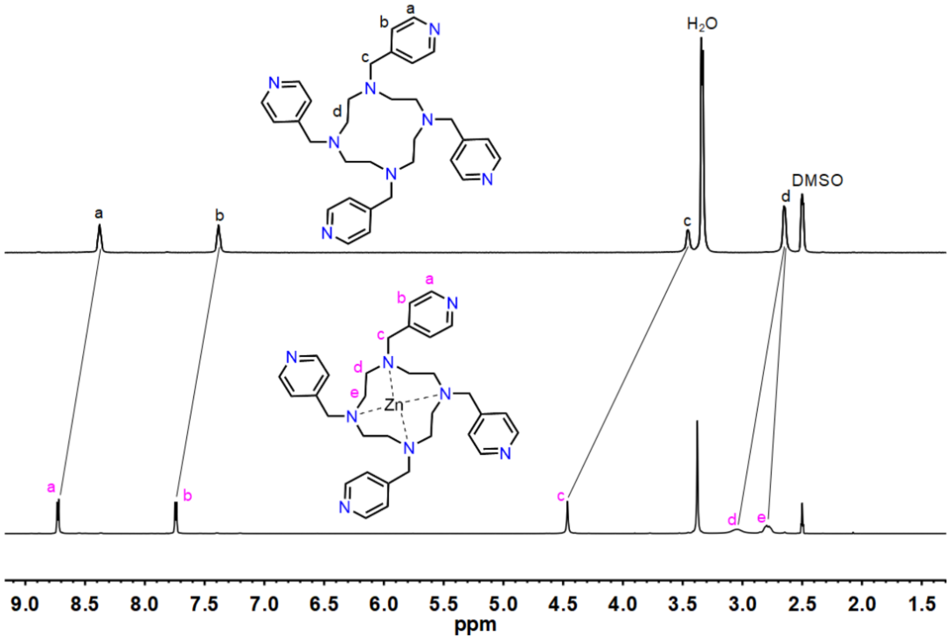

Figure S 5 The ^{1}H NMR spectra comparion between ligand **L** and **ZnL** (400 MHz, DMSO-$_{d6}$, 298 K).

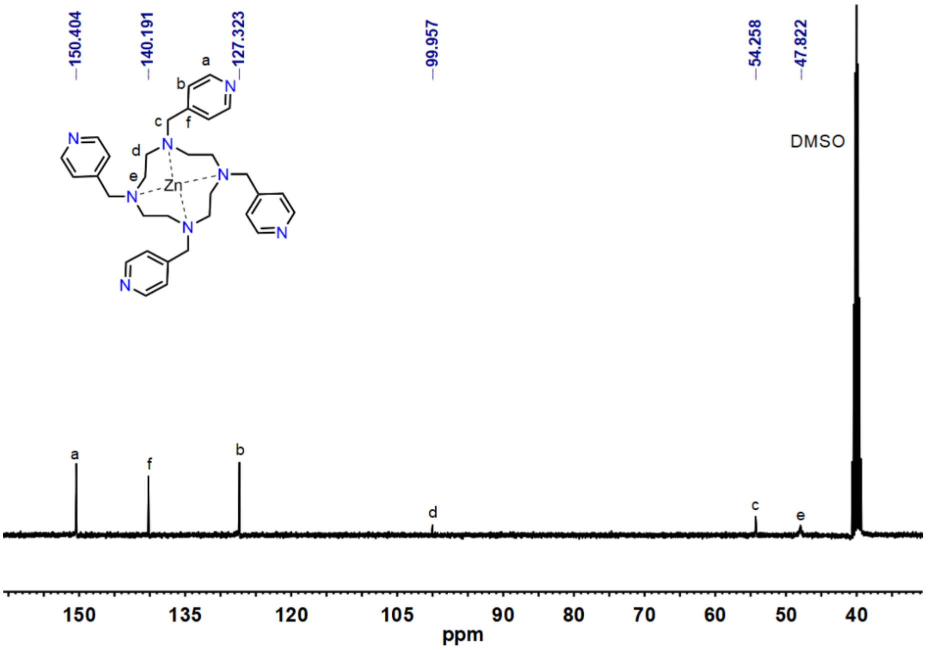

Figure S 6 The ^{13}C NMR spectrum of **ZnL** (101 MHz, DMSO-$_{d6}$, 298 K).

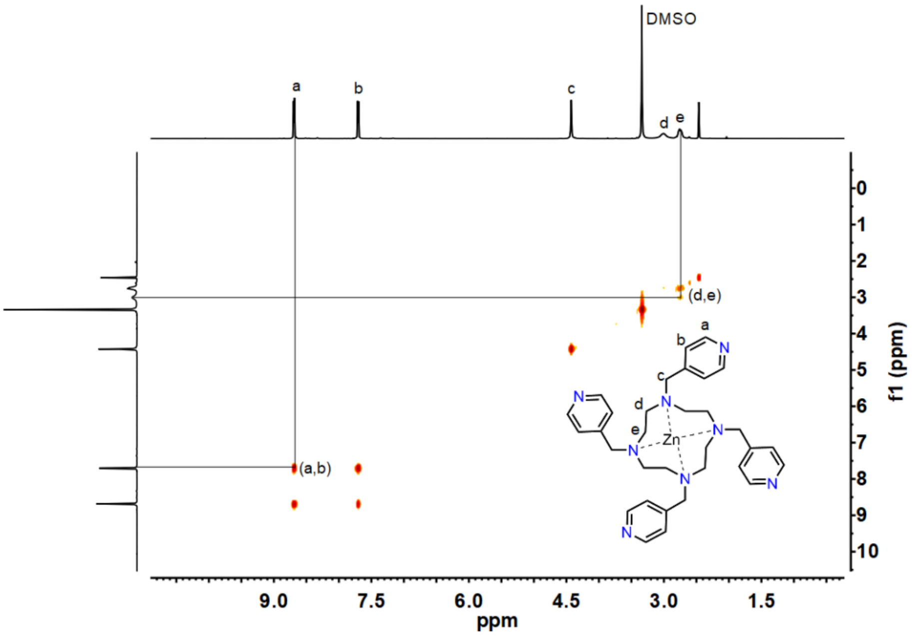

Figure S 7 The ^{1}H-^{1}H COSY spectrum of **ZnL** (400 MHz, DMSO-$_{d6}$, 298 K).

DOSY spectra

In Stokes -Einstein equation ,

$$D = \frac{k_B T}{6\pi\eta r}$$

which was applied to estimate the dynamic radius for the cage 1. D is diffusion coefficient obtained from DOSY spectrum, k_B is Boltzmann constant, T is temperature, viscosity tested to be 0.8949 mPa•s, and r is the estimated dynamic radius.

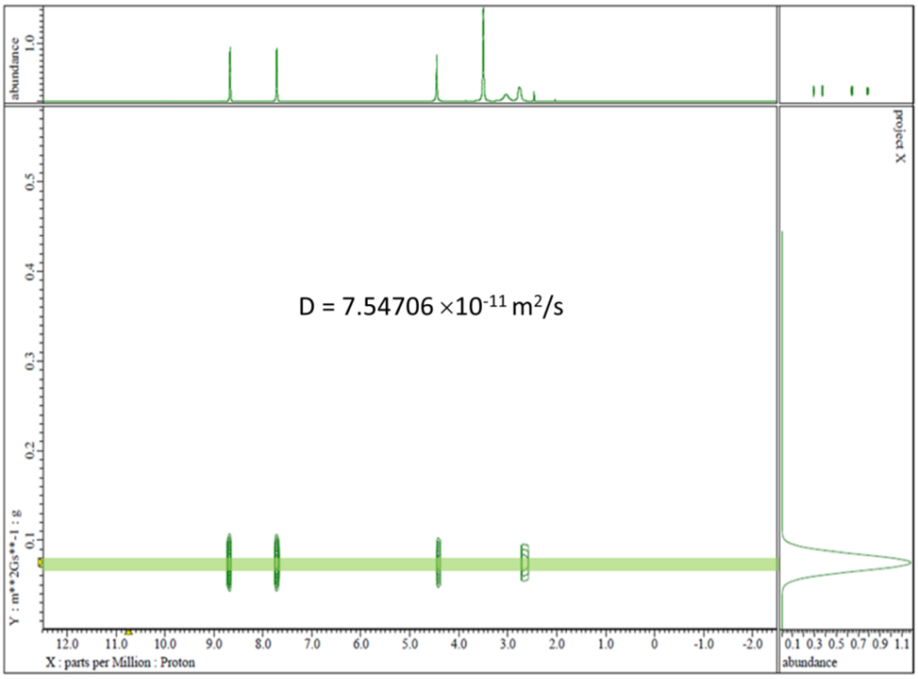

Figure S 8 The DOSY spectrum of **ZnL** (400 MHz, DMSO-$_{d6}$, 298 K). Diffusion Constant = 7.54706×10^{-11} m^2/s.

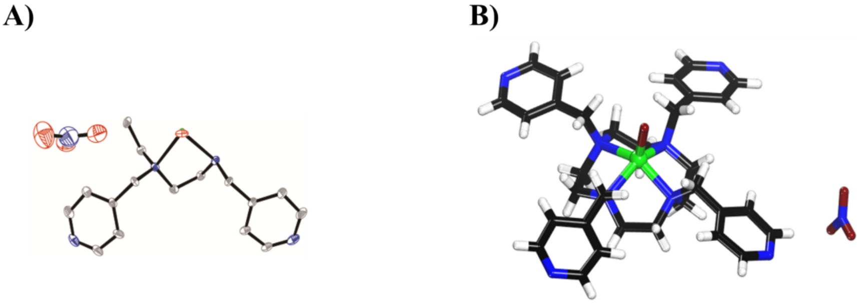

Figure S 9 The structures of **ZnL**. A) Asymmetric unit. B) The crystal structure. (balck, C; blue, N; red, O; white, H; green, Zn).

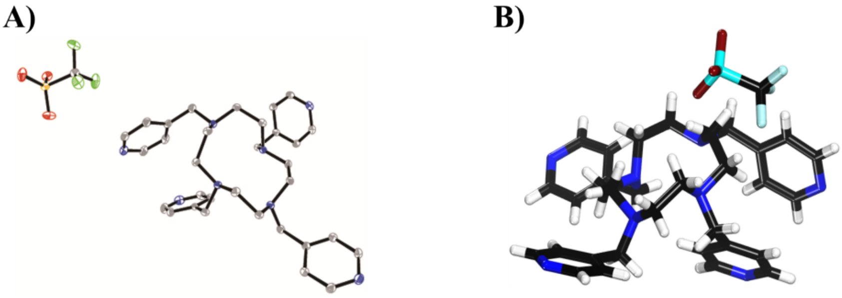

Figure S 10 The structures of Ligand **L**. A) Asymmetric unit. B) The crystal structure. (balck, C; blue, N; red, O; white, H; sky-blue, S; wathet, F).

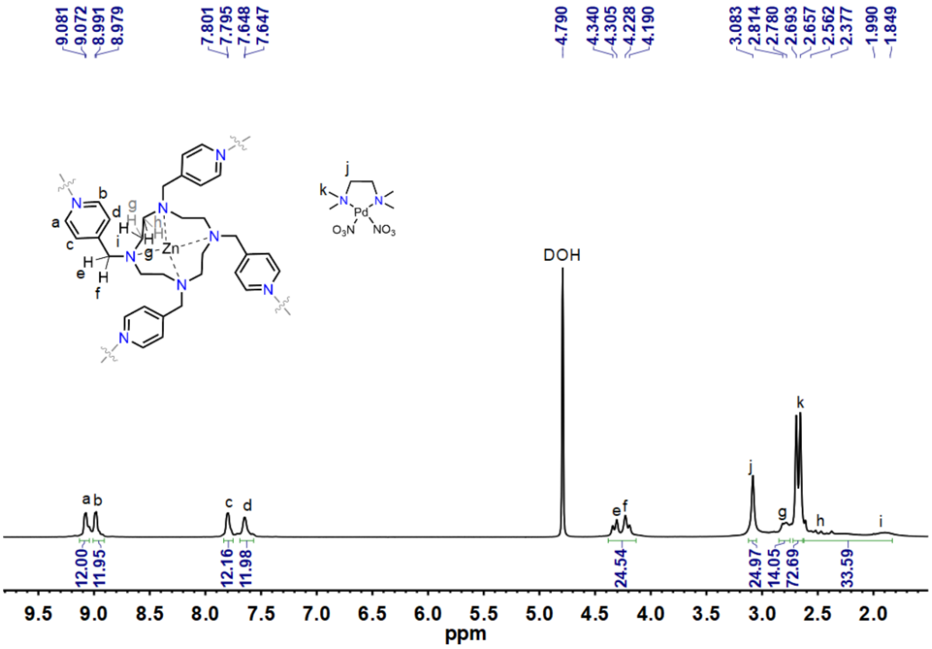

Figure S 11 The ^{1}H NMR spectrum of tube **1-Zn**(NO_3^-) (400 MHz, D_2O, 298 K).

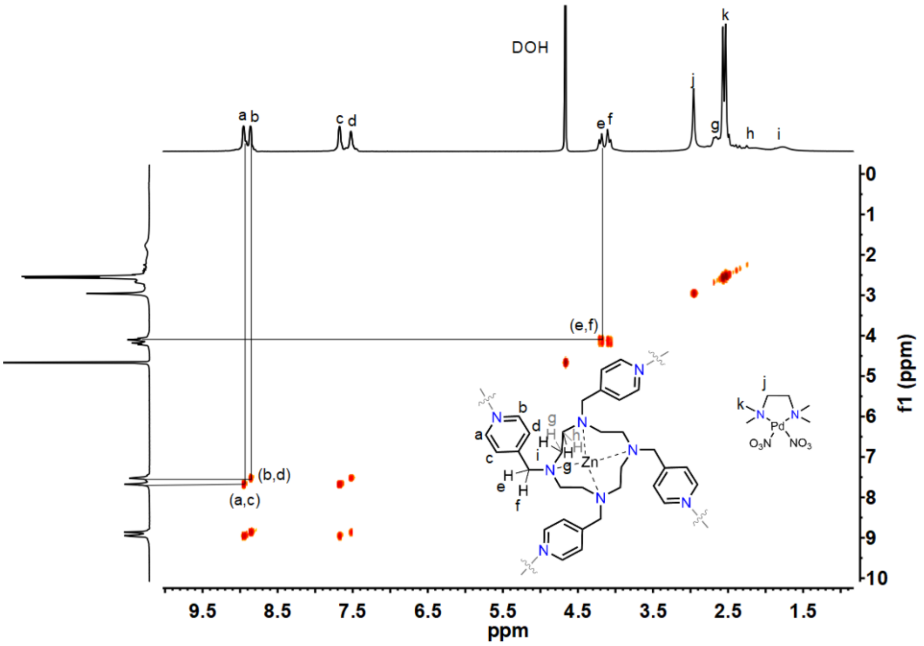

Figure S 12 The ^{1}H-^{1}H COSY spectrum of tube **1-Zn**(NO_3^-) (400 MHz, D_2O, 298 K).

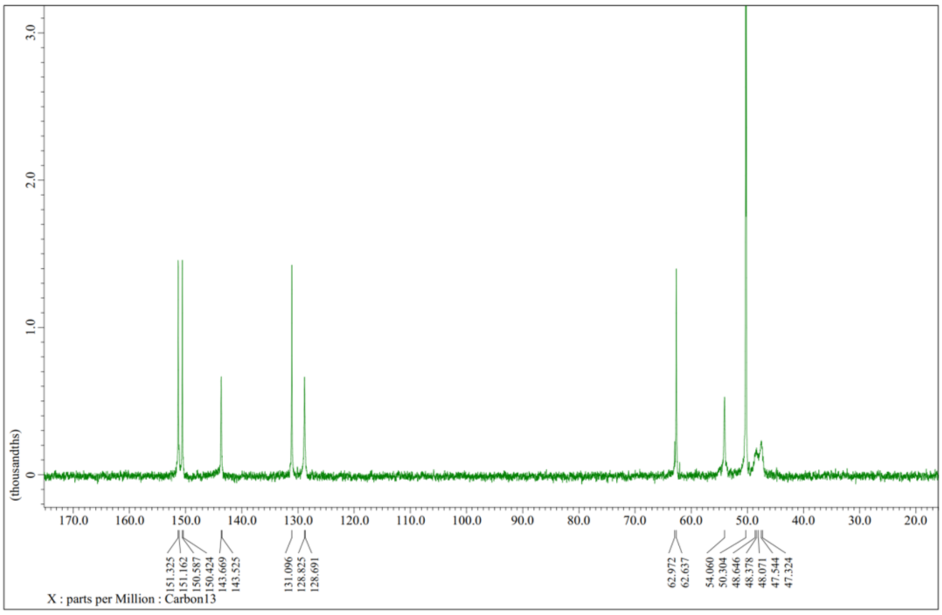

Figure S 13 The ^{13}C NMR spectrum of tube **1-Zn**(NO_3^-) (101 MHz, D_2O, 298 K).

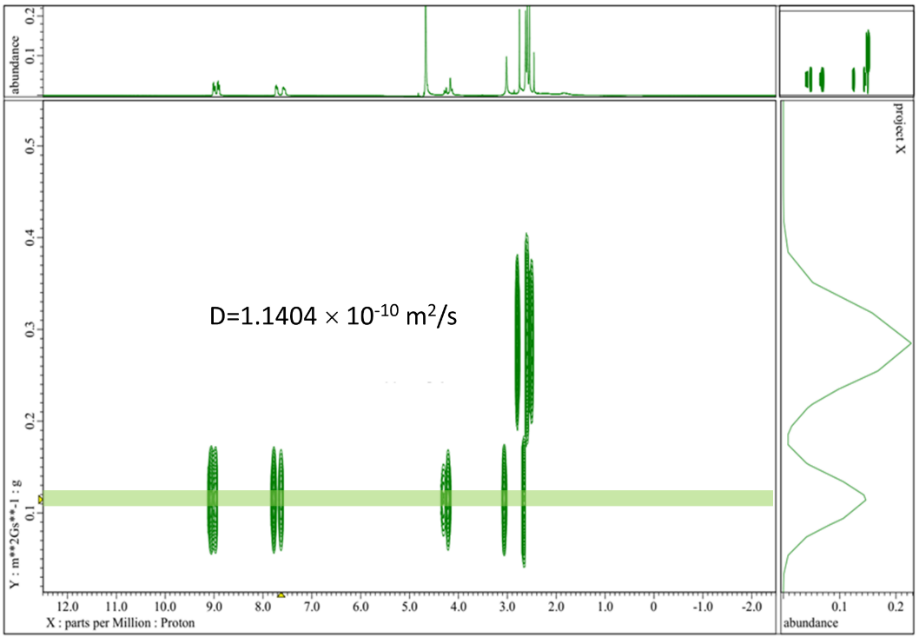

Figure S 14 The DOSY spectrum of tube **1-Zn**(NO_3^-) (400 MHz, D_2O, 298 K). Diffusion Constant = 1.1405×10^{-10} m^2/s.

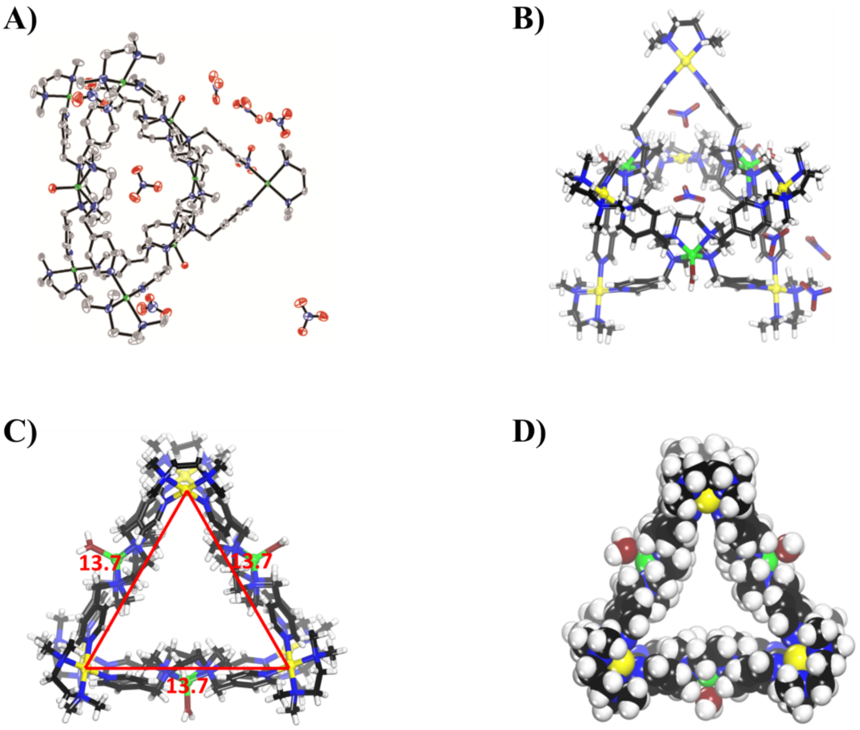

Figure S 15 The structures of tube **1-Zn**(NO_3^-). A) Asymmetric unit. B) The crystal structure. C-D) the size of tube cavity. (black, C; blue, N; yellow, Pd; red, O; green, Zn; white, H).

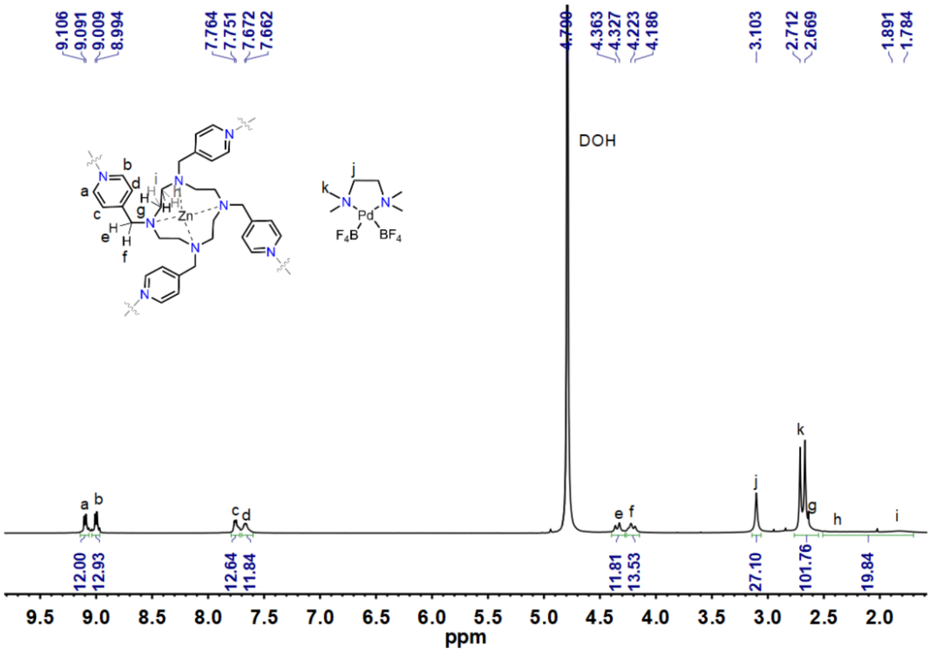

Figure S 16 The ^{1}H NMR spectrum of tube **1-Zn**-NO_3-BF_4 (400 MHz, D_2O, 298 K).

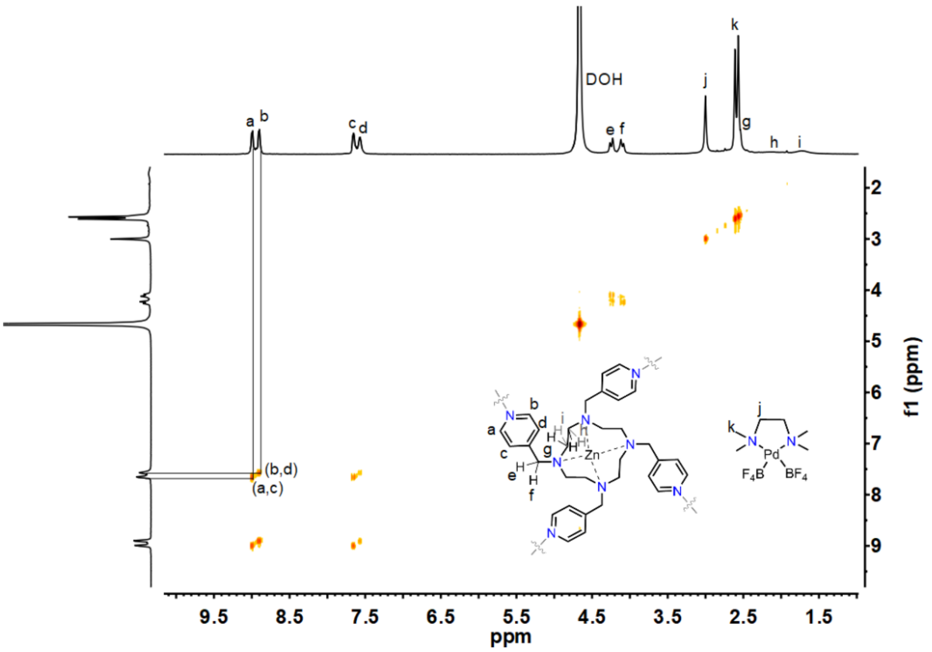

Figure S 17 The ^{1}H-^{1}H COSY spectrum of tube **1-Zn**-NO_3-BF_4 (400 MHz, D_2O, 298 K).

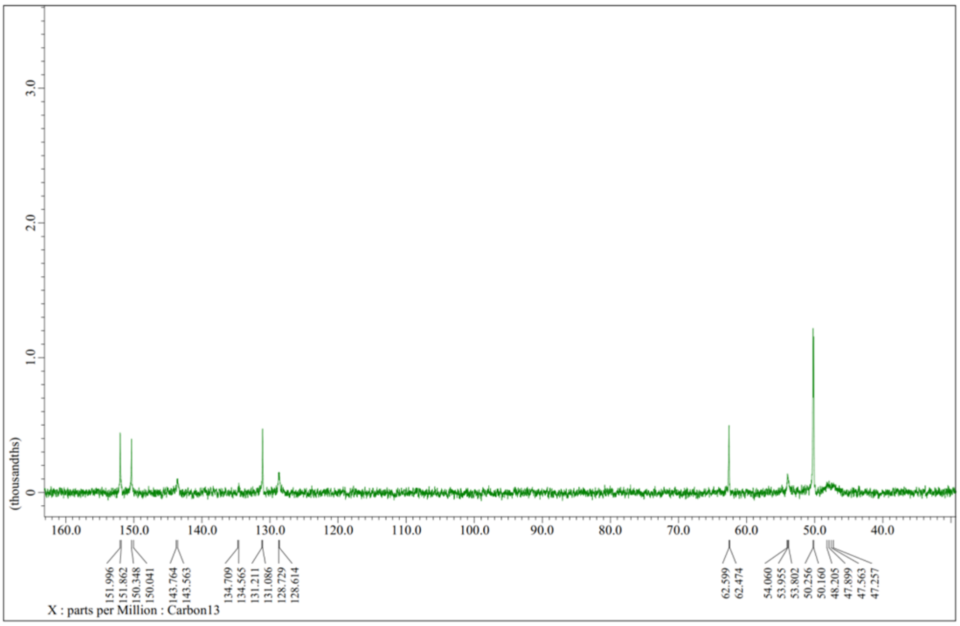

Figure S 18 The ^{13}C NMR spectrum of tube **1-Zn**-NO_3-BF_4 (101 MHz, D_2O, 298 K).

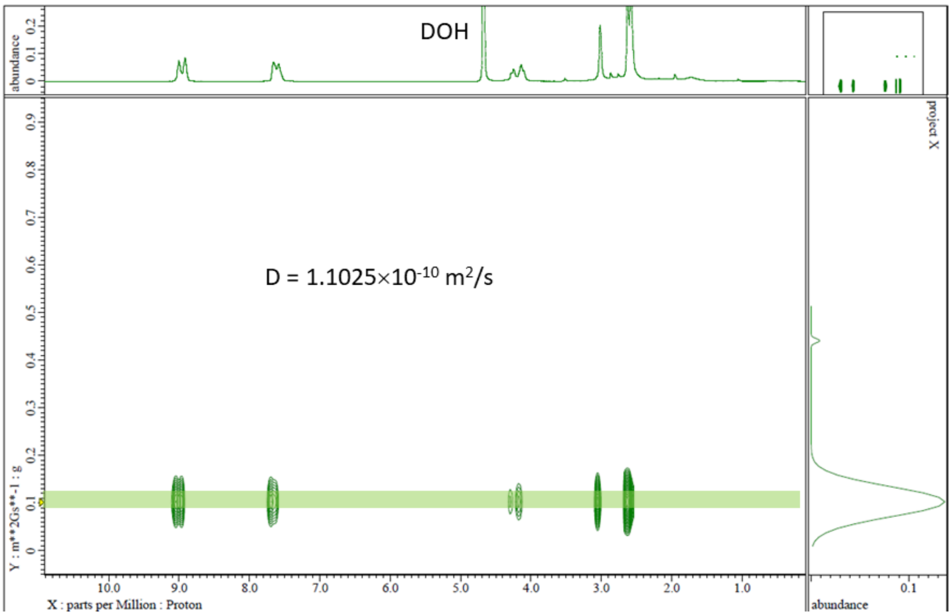

Figure S 19 The DOSY spectrum of tube **1-Zn**-NO_3-BF_4 (400 MHz, D_2O, 298 K). Diffusion Constant = 1.1025×10^{-10} m^2/s.

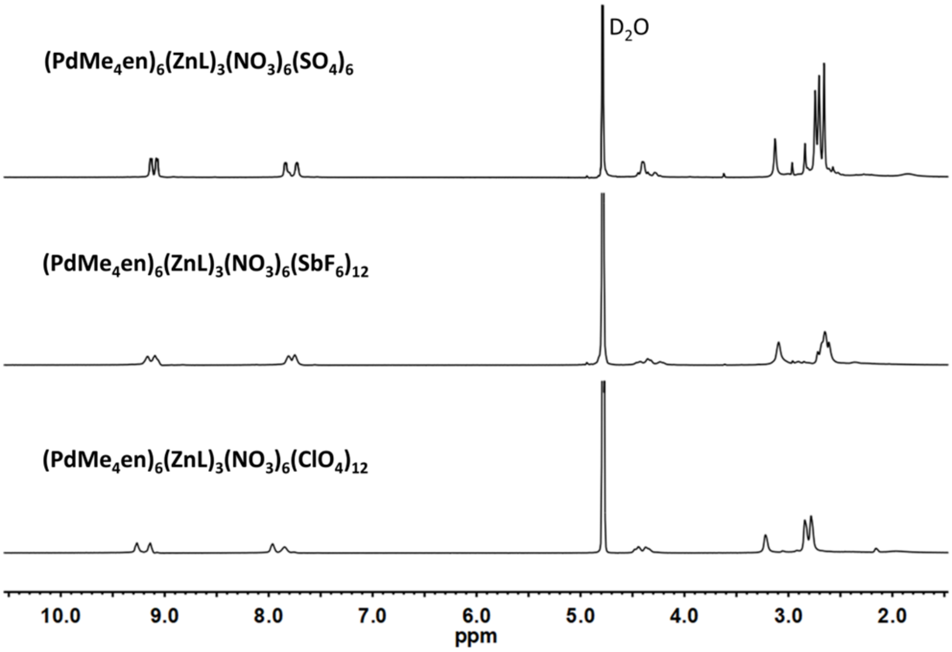

Figure S 20 The ^1H NMR spectra of other coordination tubes **1-Zn** with different anions (400 MHz, D_2O, 298 K).

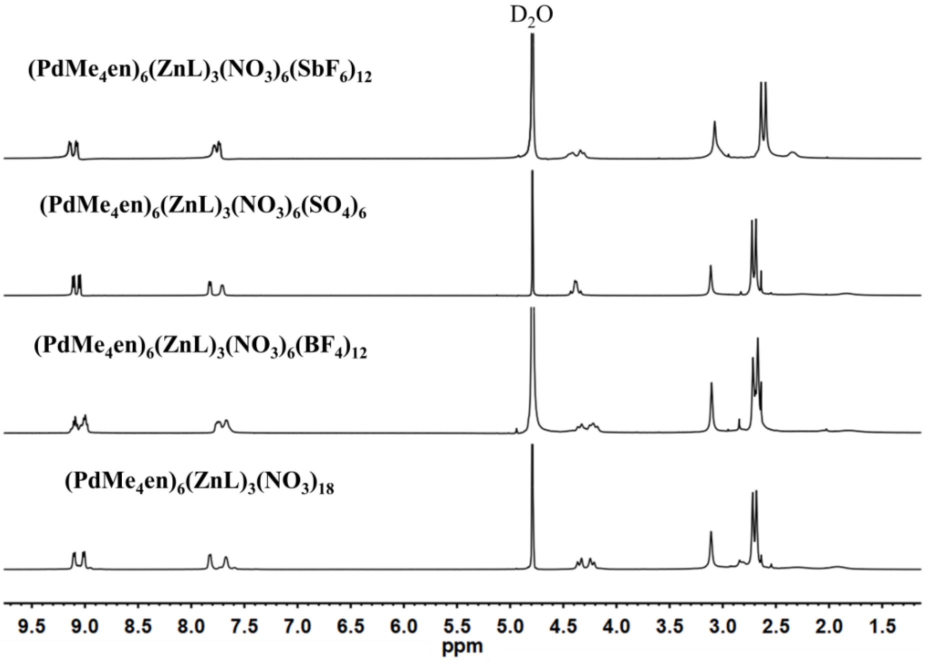

Figure S 21 The ^{1}H NMR spectra of series of coordination tubes **1-Zn** based on one pot self-assembly (400 MHz, D_2O, 298 K).

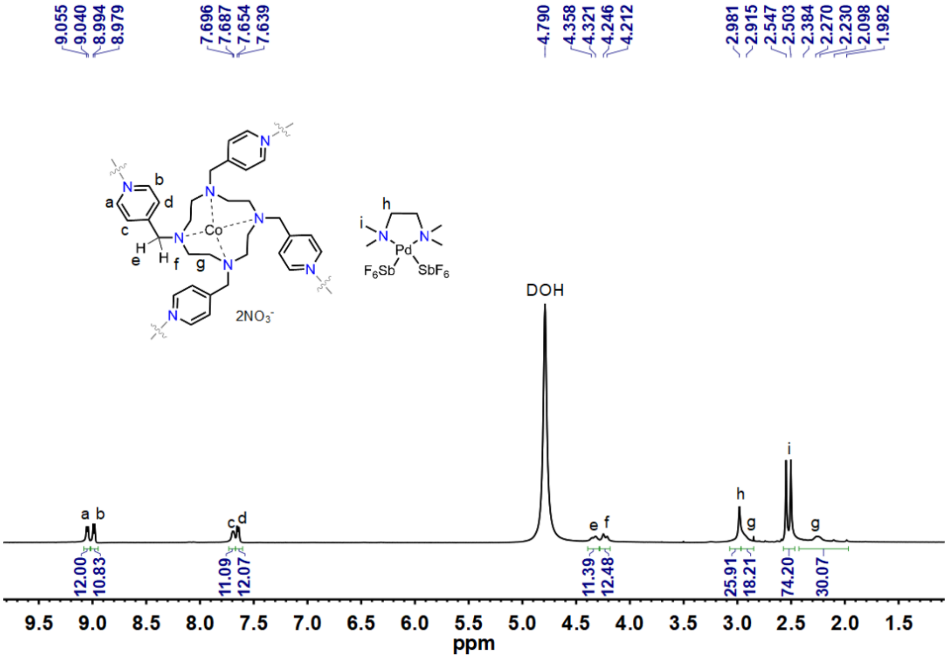

Figure S 22 The ^{1}H NMR spectrum of tube **1-Co** (400 MHz, D_2O, 298 K).

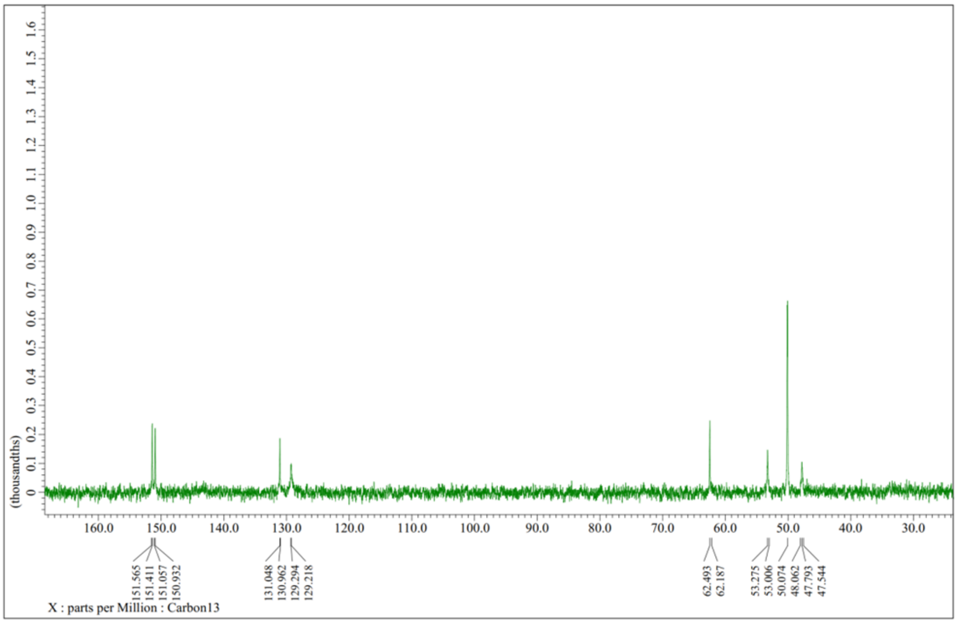

Figure S 23 The ^{13}C NMR spectrum of tube **1-Co** (101 MHz, D_2O, 298 K).

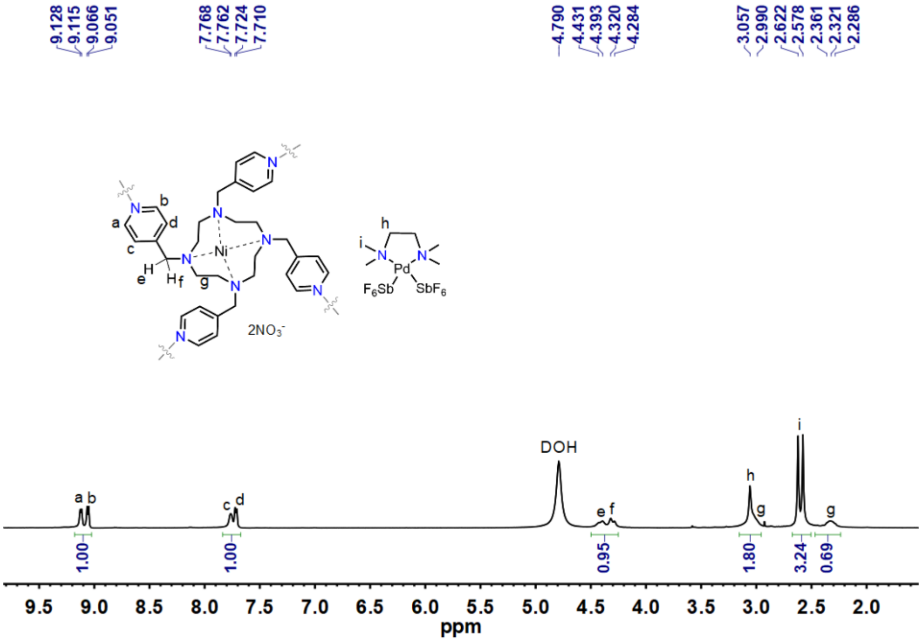

Figure S 24 The ^{1}H NMR spectrum of tube **1-Ni** (400 MHz, D_2O, 298 K).

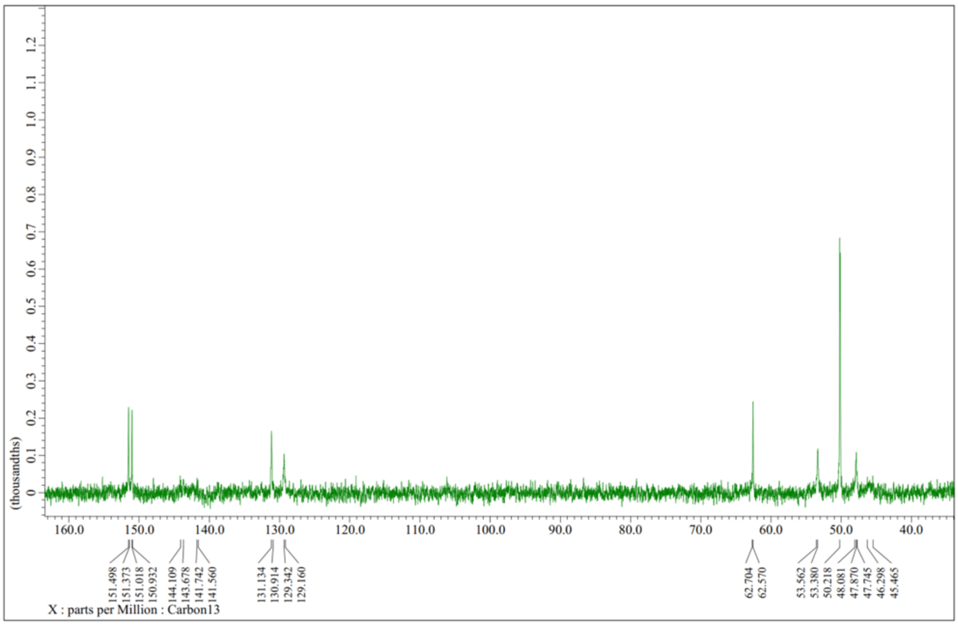

Figure S 25 The ^{13}C NMR spectrum of tube **1-Ni** (101 MHz, D_2O, 298 K).

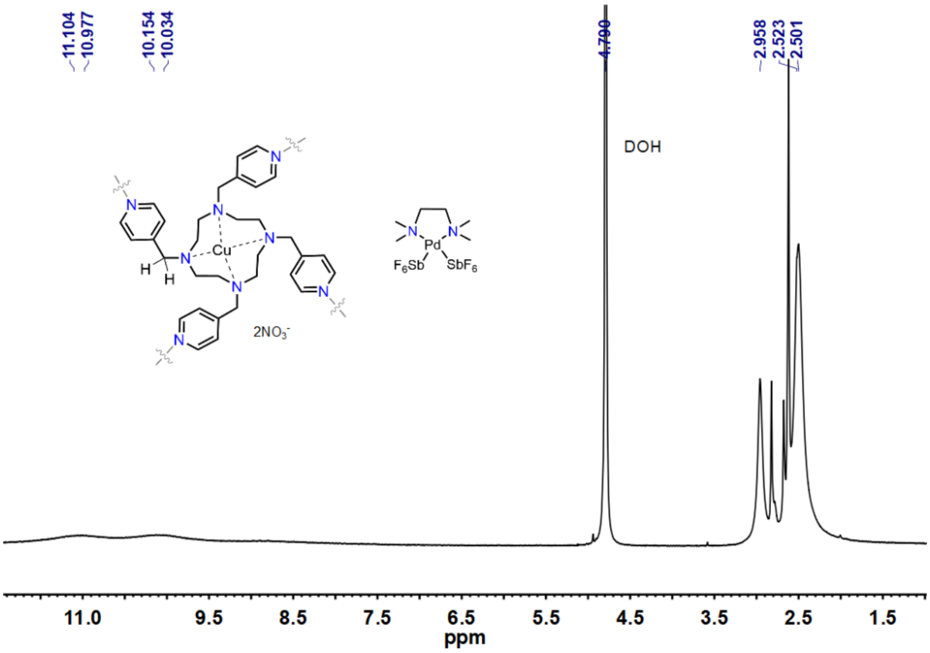

Figure S 26 The ^{1}H NMR spectrum of tube **1-Cu** (400 MHz, D_2O, 298 K).

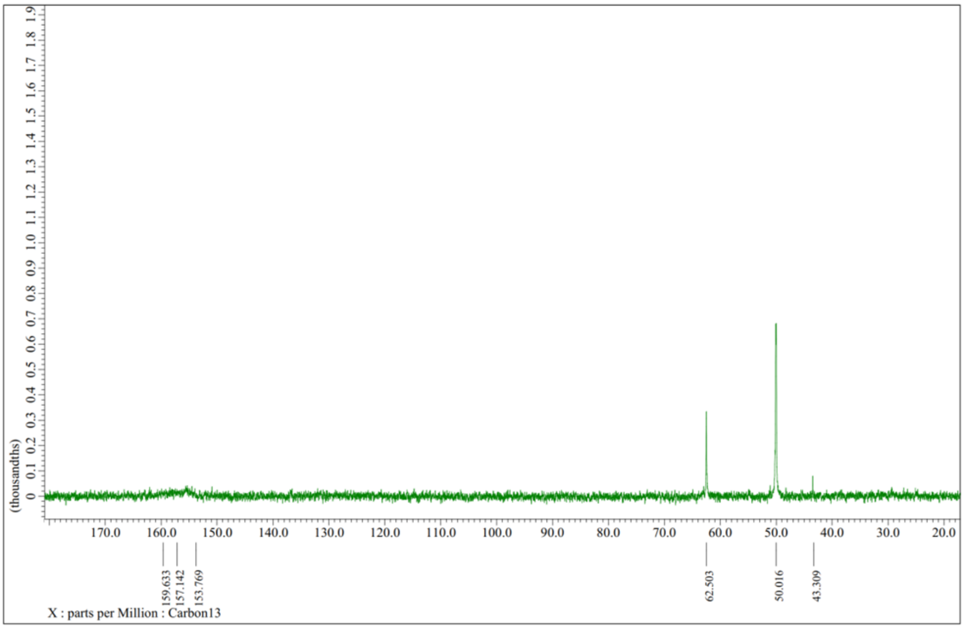

Figure S 27 The ^{13}C NMR spectrum of tube **1-Cu** (101 MHz, D_2O, 298 K).

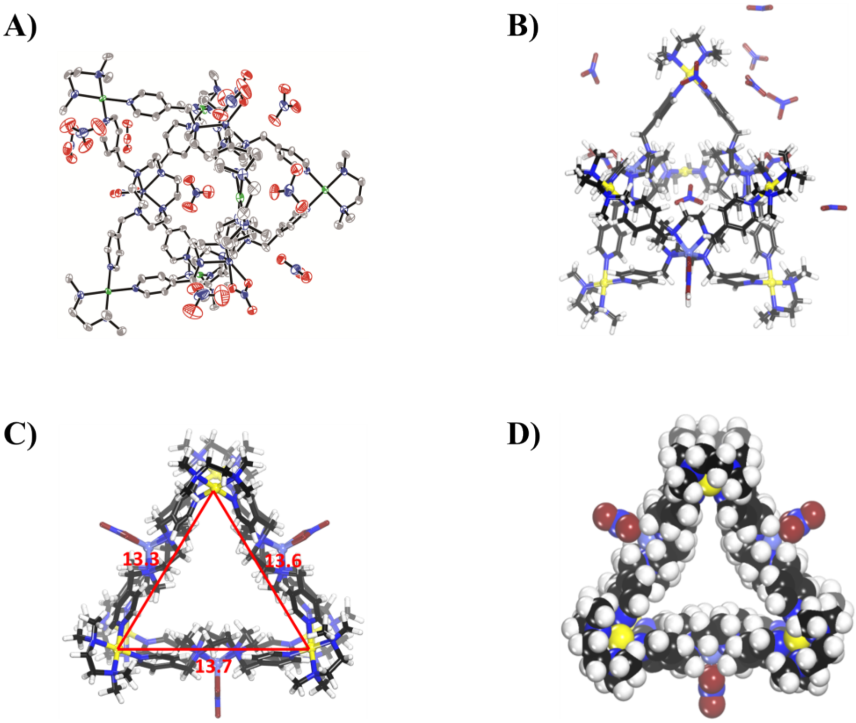

Figure S 28 The structures of tube **1-Co**. A) Asymmetric unit. B) The crystal structure. C-D) the size of tube cavity. (black, C; blue, N; yellow, Pd; red, O; bluish violet, Co; white, H).

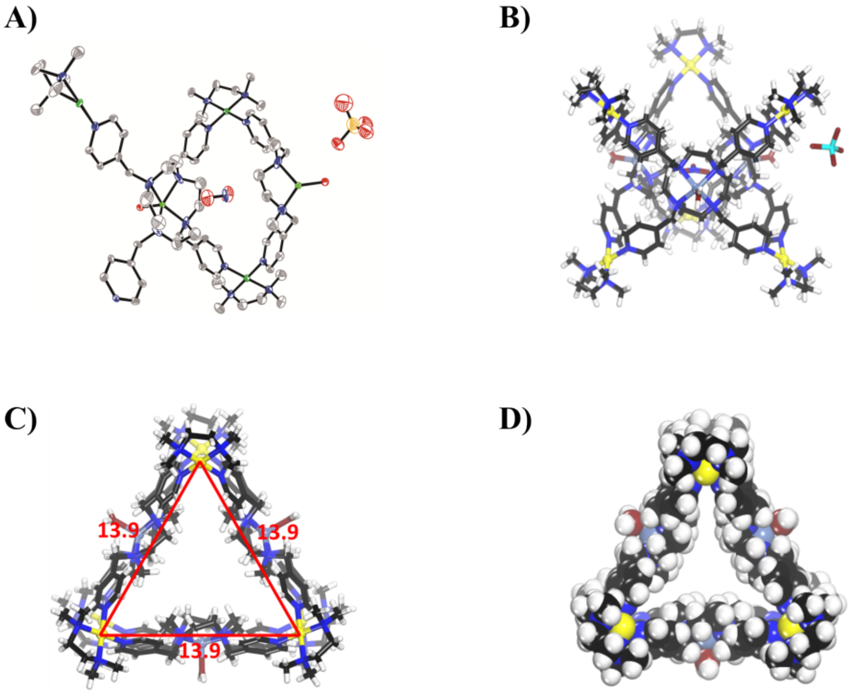

Figure S 29 The structures of tube **1-Ni**. A) Asymmetric unit. B) The crystal structure. C-D) the size of tube cavity. (black, C; blue, N; yellow, Pd; red, O; dusty blue, Ni; sky-blue, S; white, H).

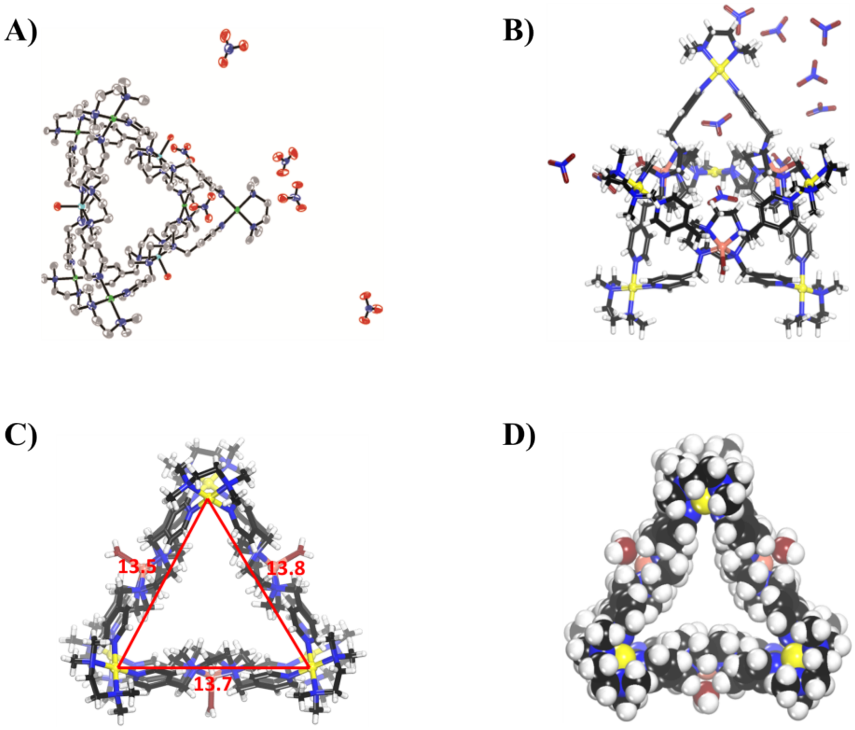

Figure S 30 The structures of tube **1-Cu**. A) Asymmetric unit. B) The crystal structure. C-D) the size of tube cavity. (black, C; blue, N; yellow, Pd; red, O; orangered, Cu; white, H).

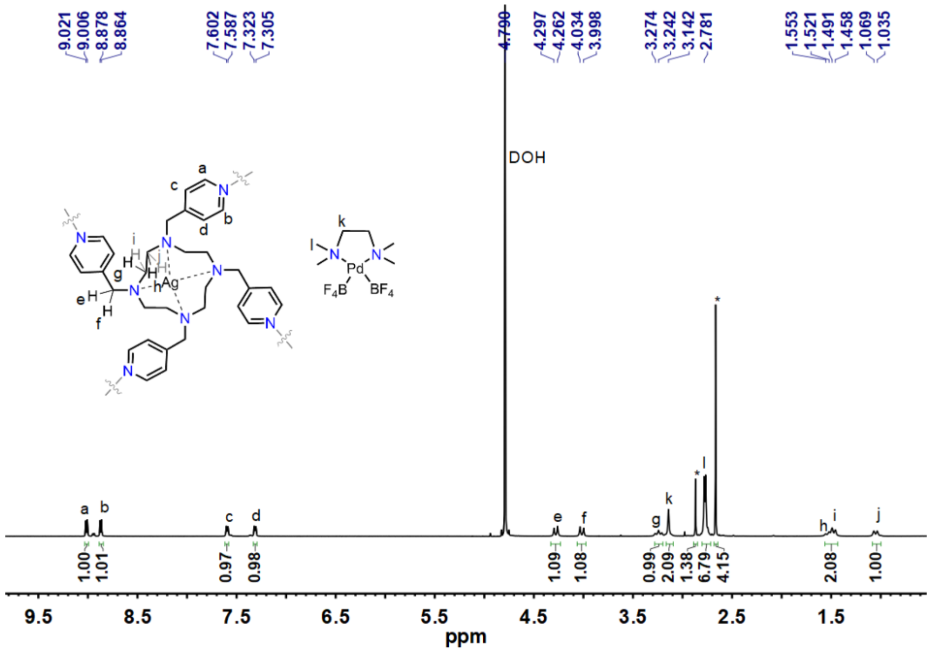

Figure S 31 The ^1H NMR spectrum of cage **2**(BF_4^-) (400 MHz, D_2O, 298 K).

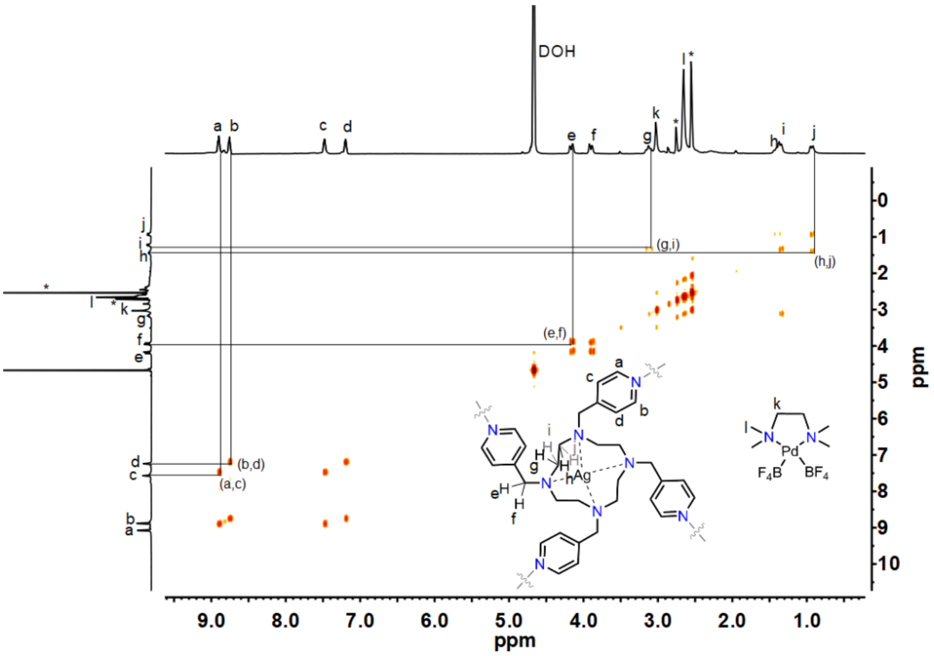

Figure S 32 The ^1H-^1H COSY spectrum of cage **2**(BF_4^-) (400 MHz, D_2O, 298 K).

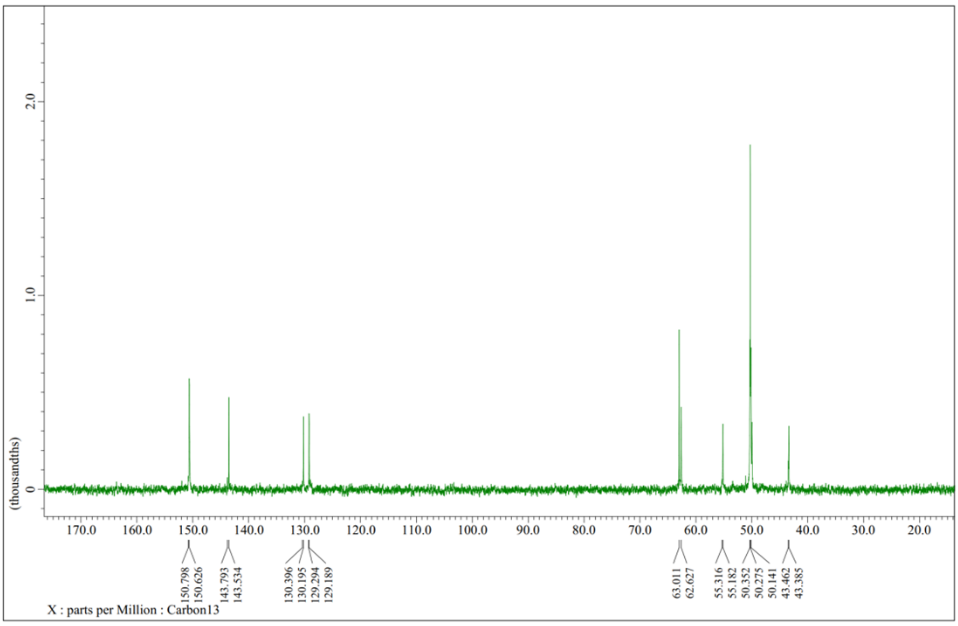

Figure S 33 The ^{13}C NMR spectrum of cage **2**(BF_4^-) (101 MHz, D_2O, 298 K).

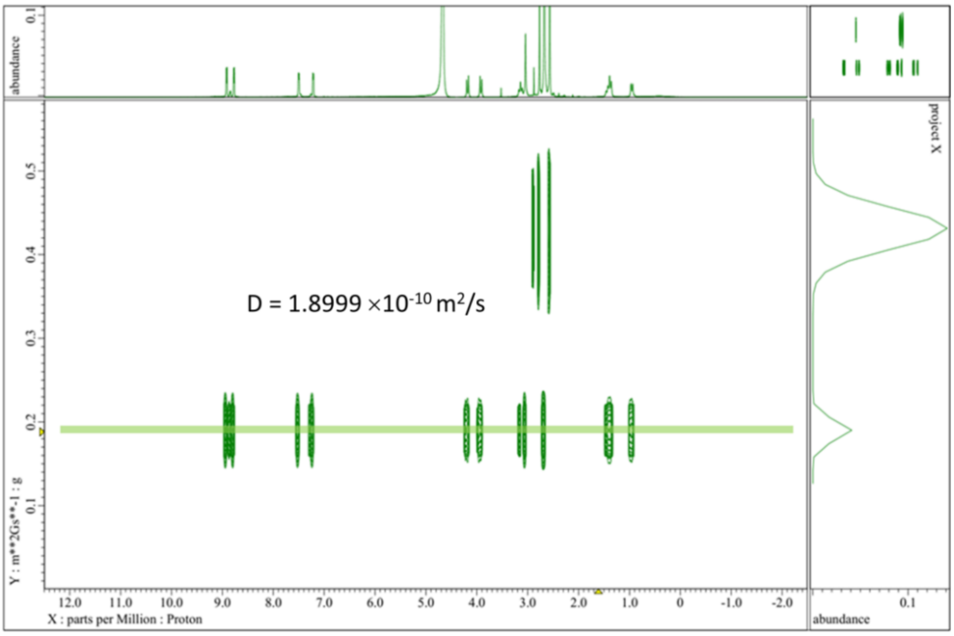

Figure S 34 The DOSY spectrum of cage **2**(BF_4^-) (400 MHz, D_2O, 298 K). Diffusion Constant = 1.8999×10$^{\mathbf{-10}}$ m$^{\mathbf{2}}$/s.

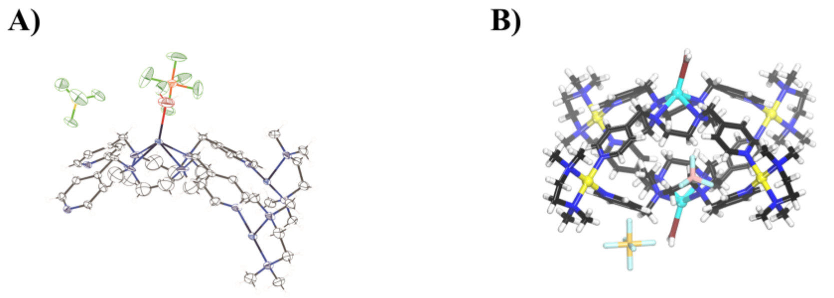

Asymmetric unit

Complete crystal structure

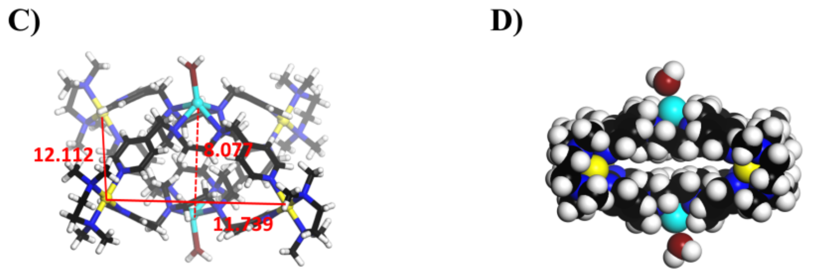

Size of window

Vision of window

Figure S 35 The structures of cage **2**(BF_4^-). A) Asymmetric unit. B) The crystal structure. C-D) the size of cage cavity. (black, C; blue, N; red, O; yellow, Pd; pale blue, Ag; white, H; wathet, F; orange, Si).

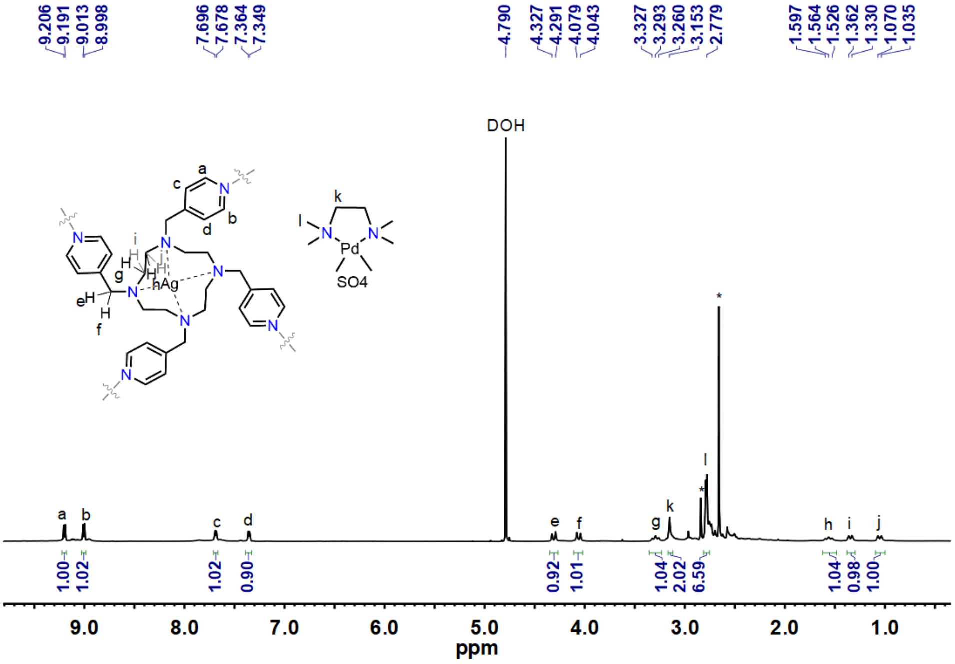

Figure S 36 The ^{1}H NMR spectrum of cage **2**(SO_4^{2-}) (400 MHz, D_2O, 298 K).

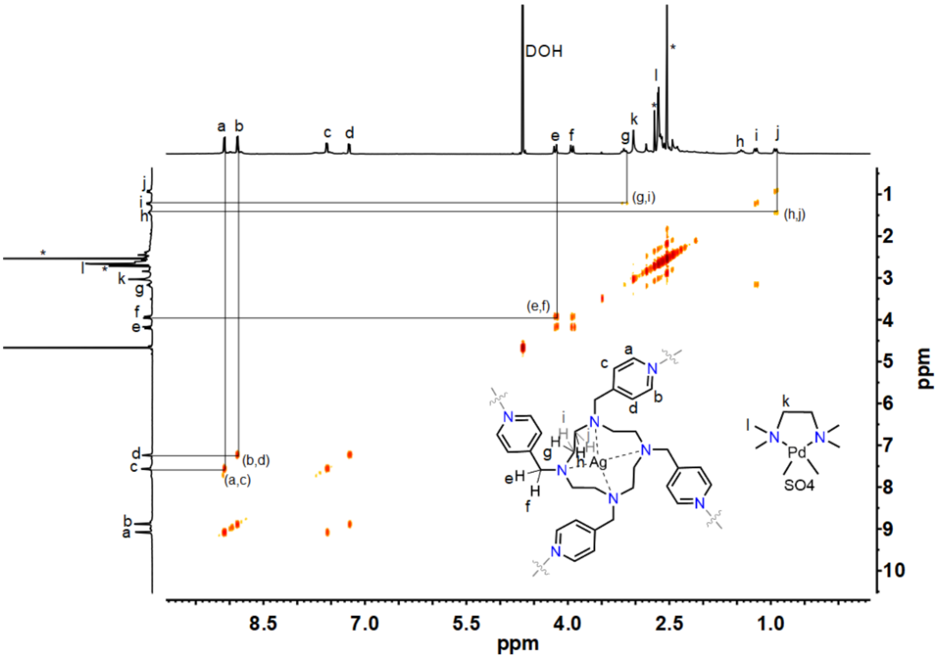

Figure S 37 The ^{1}H-^{1}H COSY spectrum of cage **2**(SO_4^{2-}) (400 MHz, D_2O, 298 K).

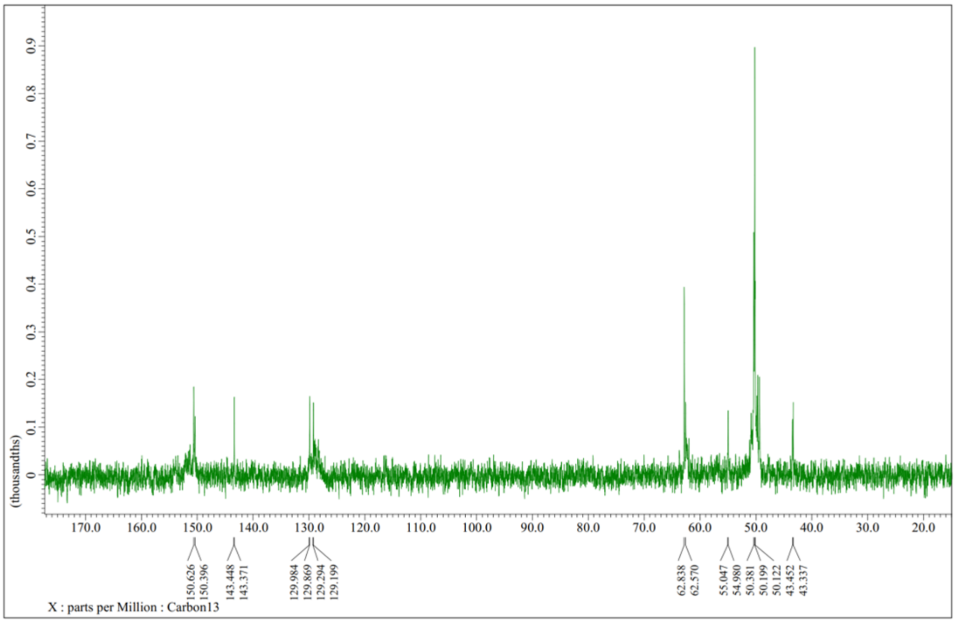

Figure S 38 The ^{13}C NMR spectrum of cage **2**(SO_4^{2-}) (101 MHz, D_2O, 298 K).

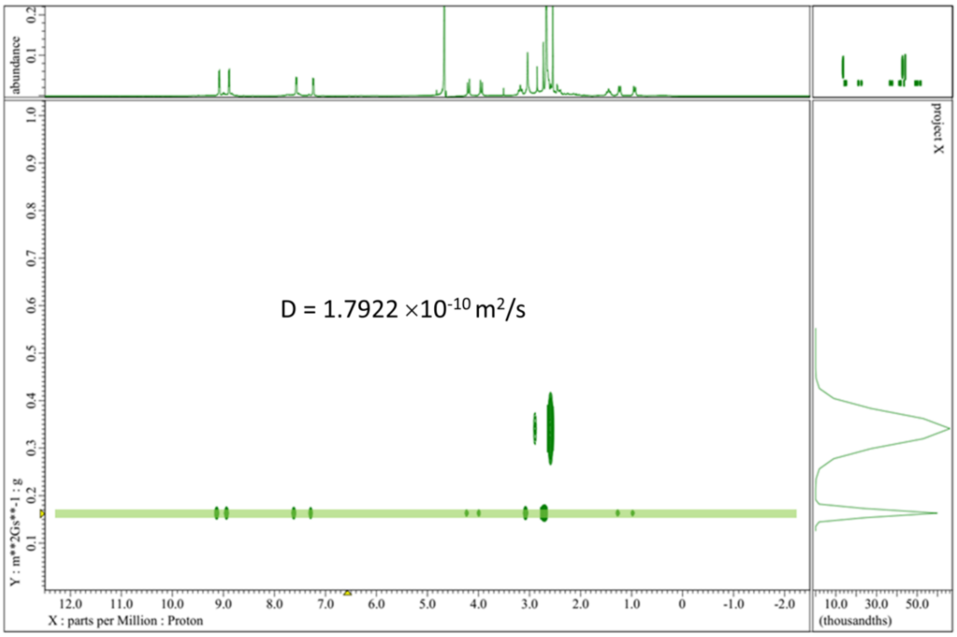

Figure S 39 The DOSY spectrum of of cage **2**(SO_4^{2-}) (400 MHz, D_2O, 298 K). Diffusion Constant = 1.7922×10^{-10} m^2/s.

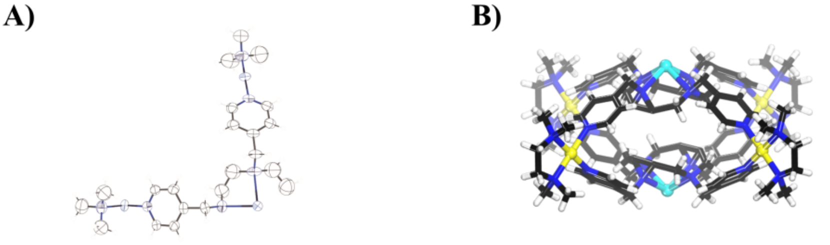

Asymmetric unit

Complete crystal structure

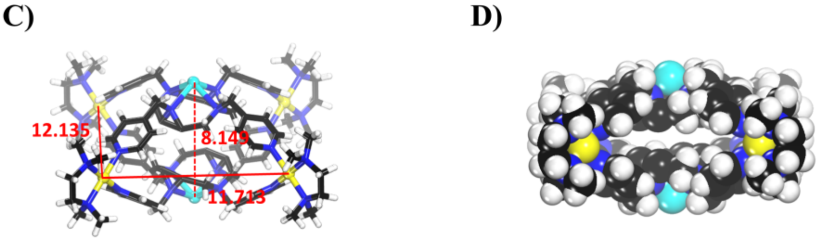

Size of window

Vision of window

Figure S 40 The structures of cage **2**(SO_4^{2-}). A) Asymmetric unit. B) The crystal structure. C-D) the size of cage cavity. (black, C; blue, N; yellow, Pd; pale blue, Ag; white, H).

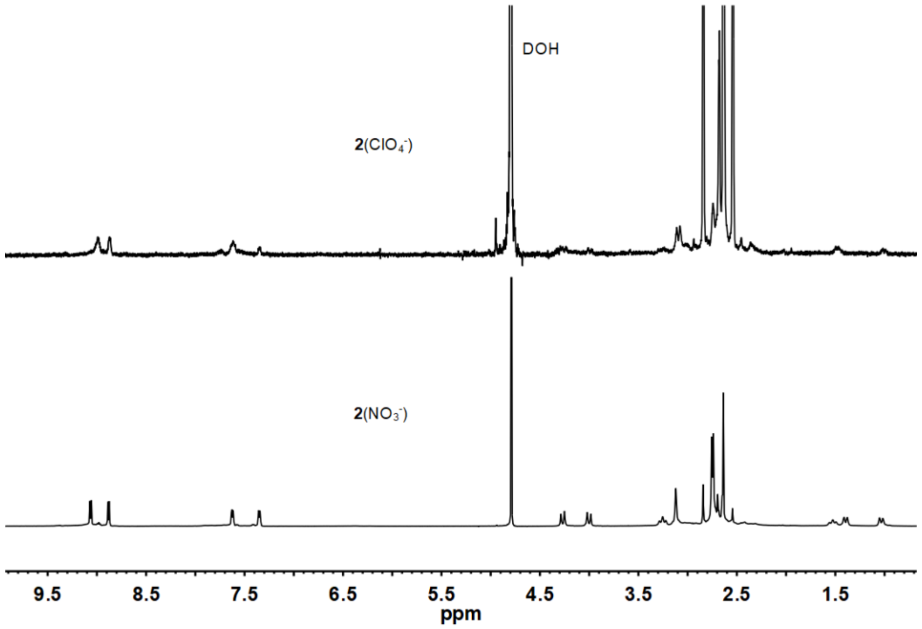

Figure S 41 The ^{1}H NMR spectra of other anionic cage **2** (400 MHz, D_2O, 298 K).

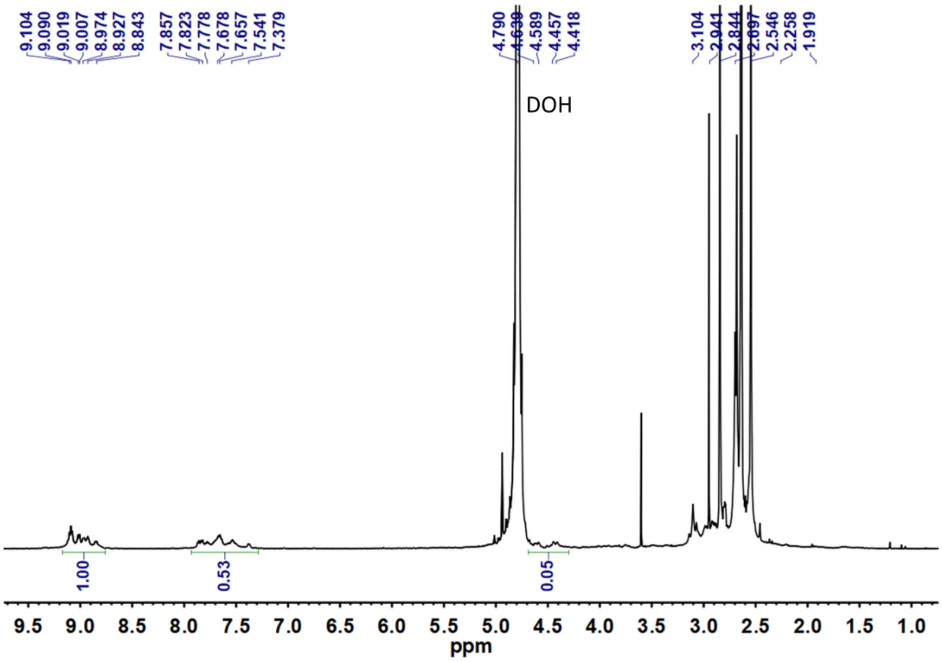

Figure S 42 The ^{1}H-NMR spectrum of coordination complex based on **L** and $Me_4en\text{-}Pd(NO_3)_2$ (400 MHz, D_2O, 298 K).

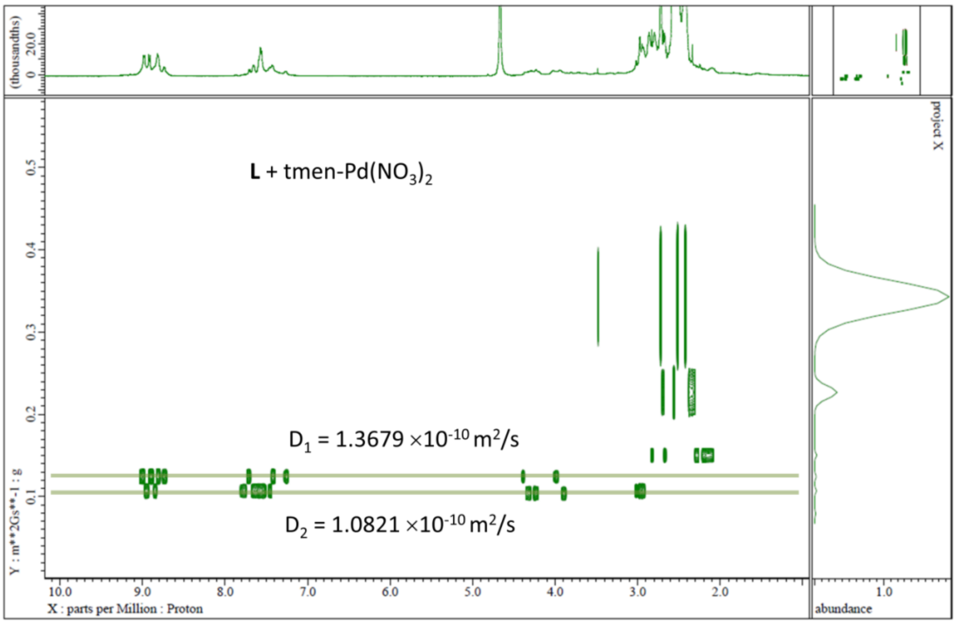

Figure S 43 The DOSY spectrum of coordination complex based on **L** and Me_4en-Pd$(NO_3)_2$ (400 MHz, D_2O, 298 K).

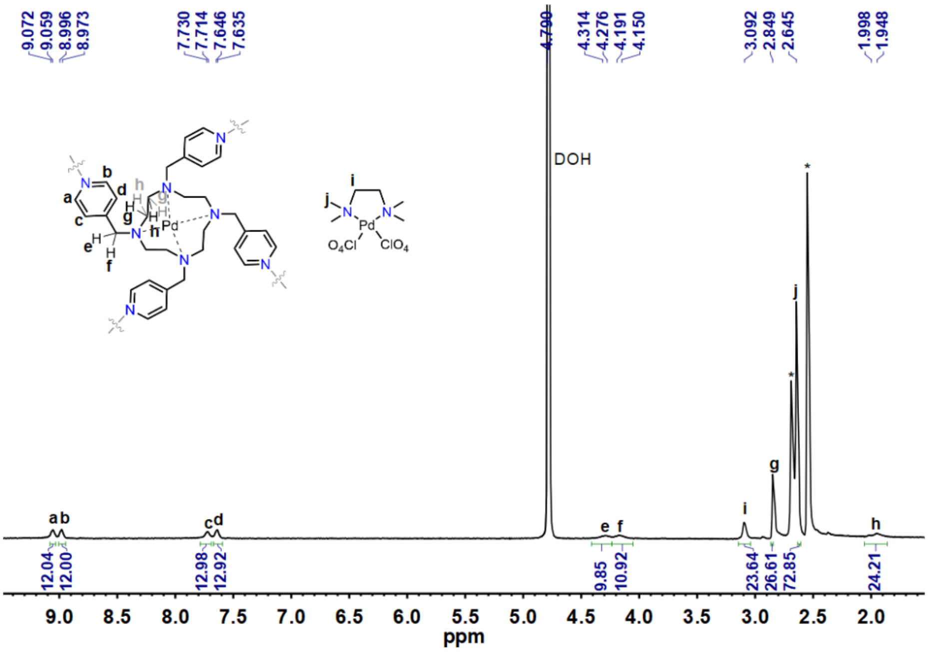

Figure S 44 The ^{1}H NMR spectrum of tube **3**(ClO_4^-) (400 MHz, D_2O, 298 K).

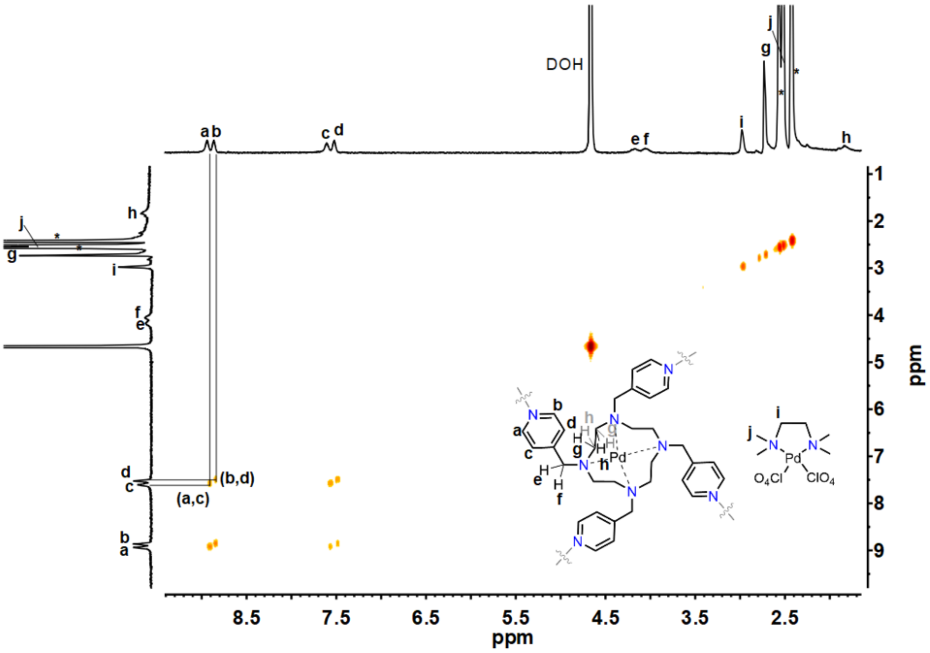

Figure S 45 The ^{1}H-^{1}H COSY spectrum of tube **3**(ClO_4^-) (400 MHz, D_2O, 298 K).

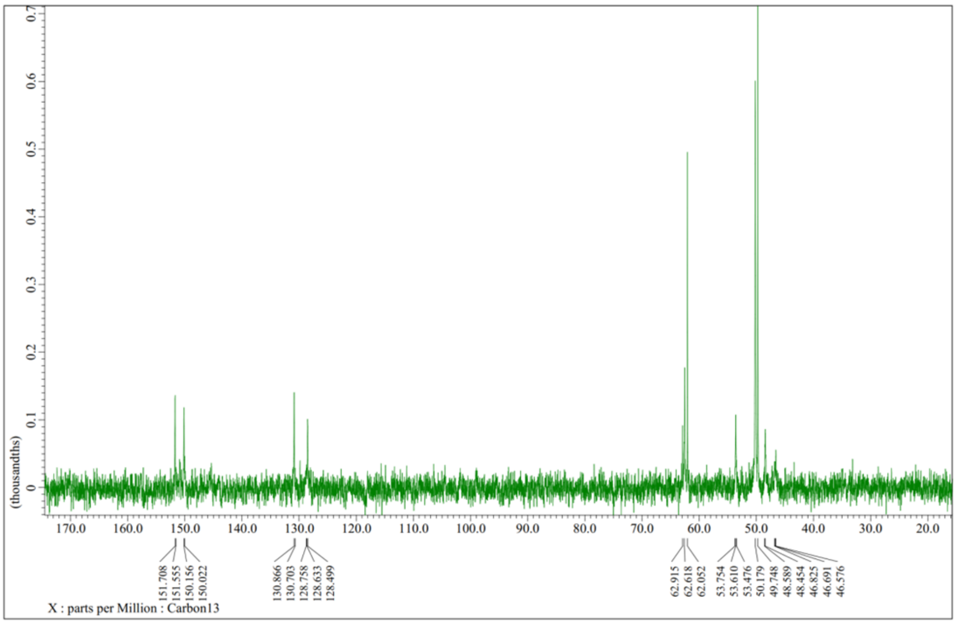

Figure S 46 The ^{13}C NMR spectrum of tube **3**(ClO_4^-) (101 MHz, D_2O, 298 K).

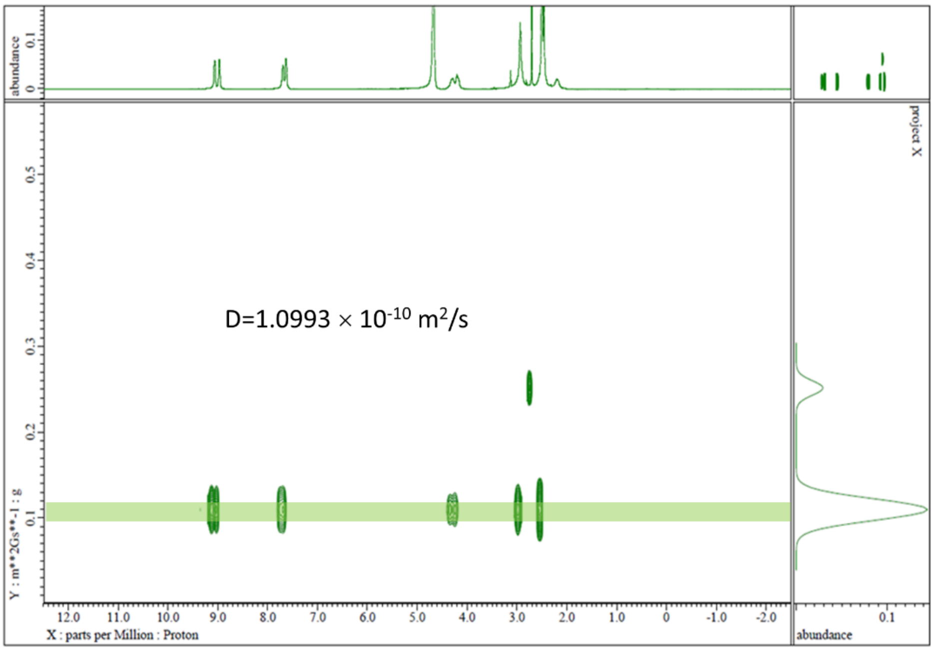

Figure S 47 The DOSY spectrum of tube **3**(ClO_4^-) (400 MHz, D_2O, 298 K). Diffusion Constant = 1.0993×10^{-10} m^2/s.

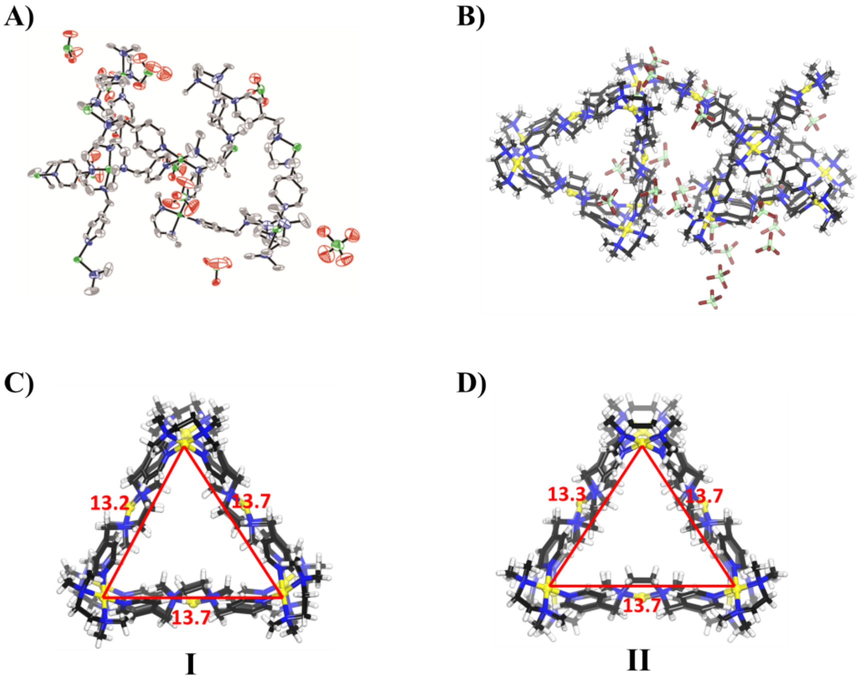

Figure S 48 The structures of tube **3**(ClO_4^-). A) Asymmetric unit. B) The crystal structure. C-D) the sizes of tube cavity I and II. (black, C; blue, N; yellow, Pd; red, O; cyan, Cl; white, H).

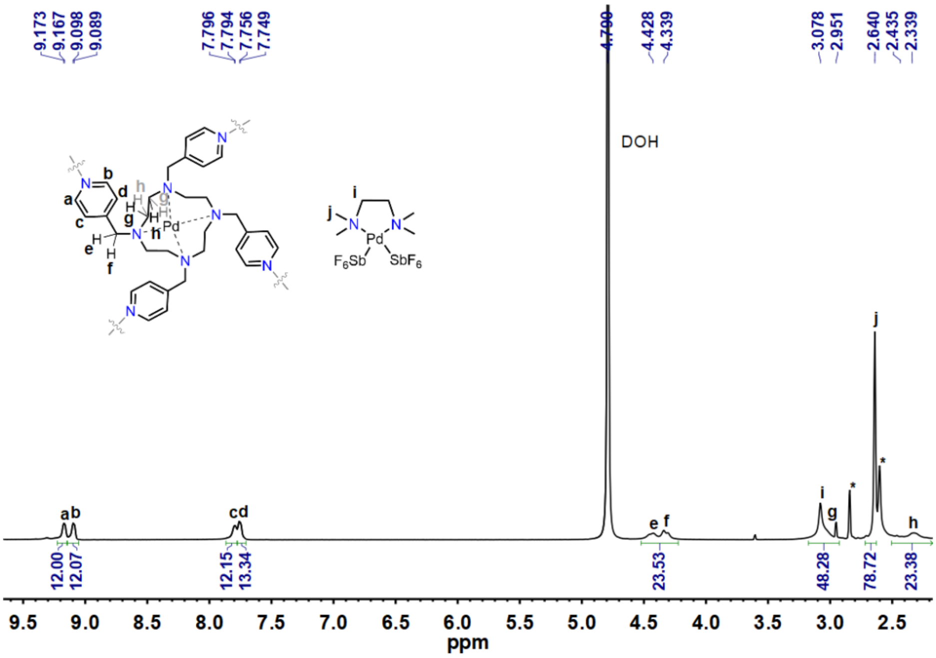

Figure S 49 The ^{1}H NMR spectrum of tube **3**(SbF_6^-) (400 MHz, D_2O, 298 K).

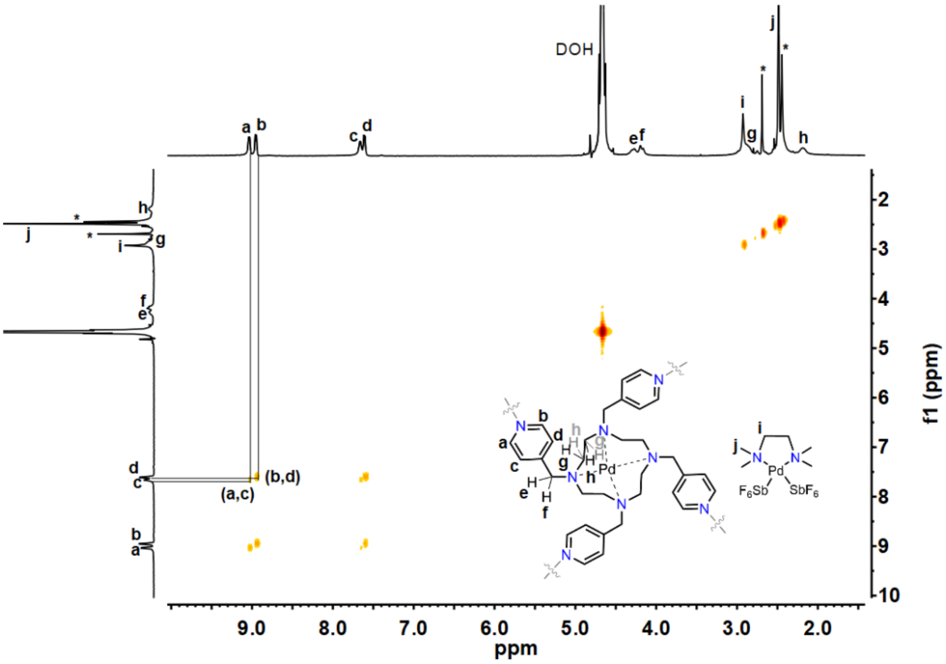

Figure S 50 The ^{1}H-^{1}H COSY spectrum of tube **3**(SbF_6^-) (400 MHz, D_2O, 298 K).

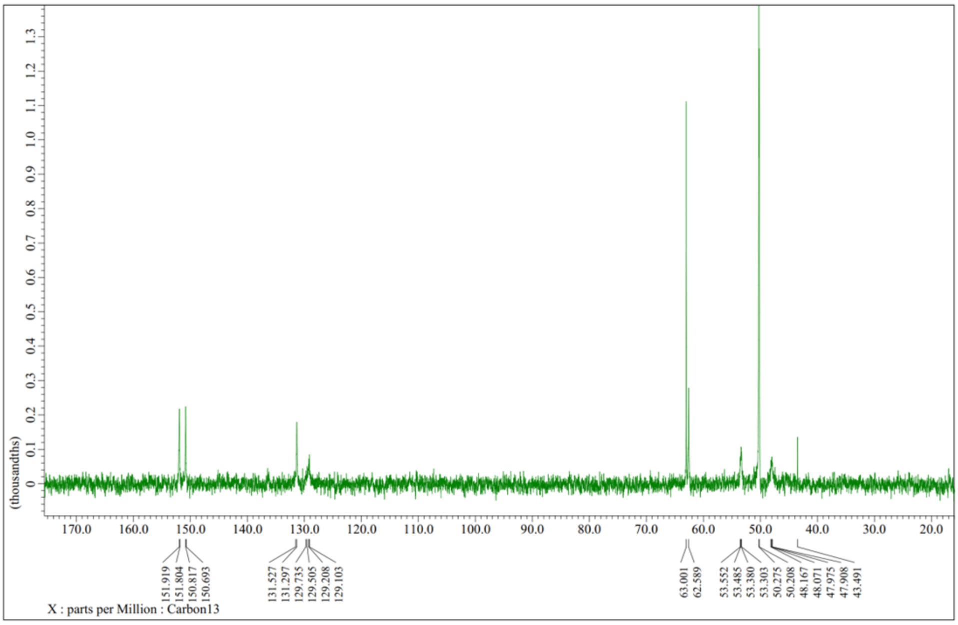

Figure S 51 The ^{13}C NMR spectrum of tube **3**(SbF_6^-) (101 MHz, D_2O, 298 K).

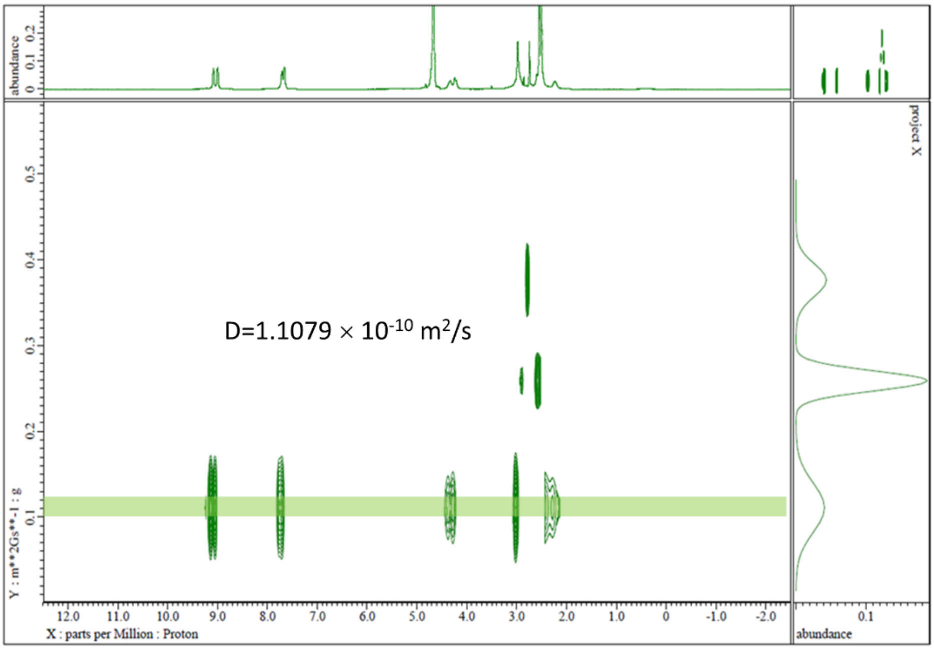

Figure S 52 The DOSY spectrum of tube **3**(SbF_6^-) (400 MHz, D_2O, 298 K). Diffusion Constant = 1.1079×10^{-10} m^2/s.

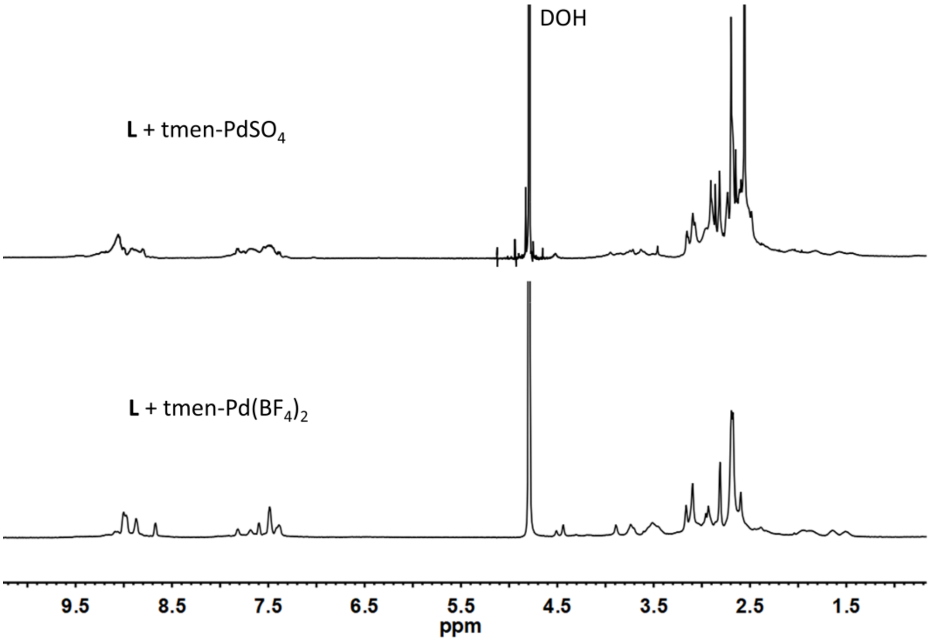

Figure S 53 The ^{1}H NMR spectra of complexes based on ligand **L** and $Me_4enPd(BF_4)_2$/ $Me_4enPdSO_4$ (400 MHz, D_2O, 298 K).

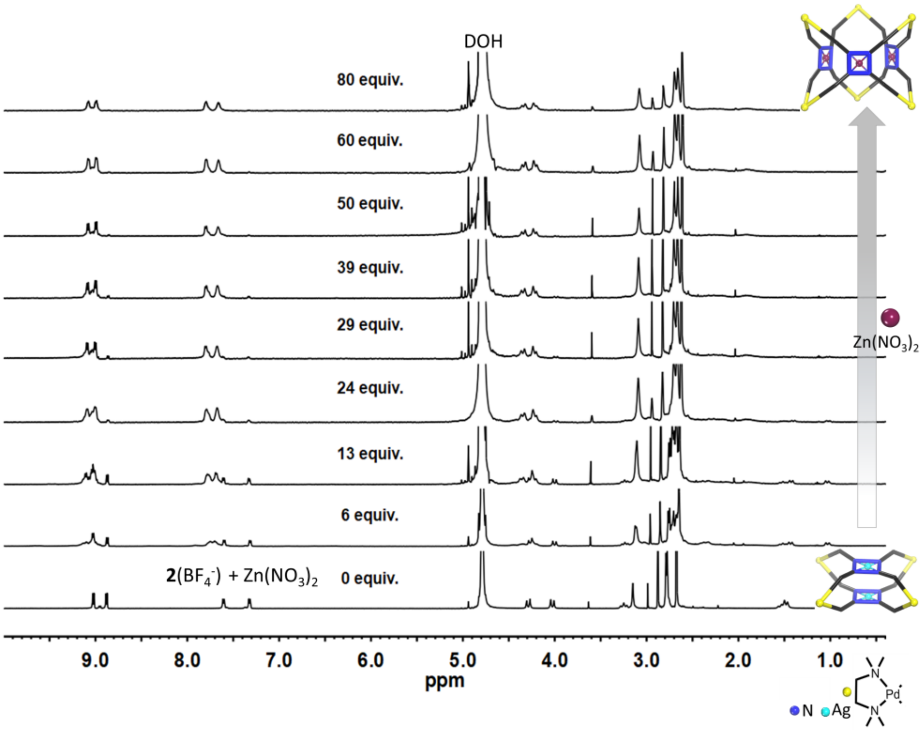

Figure S 54 The ^{1}H NMR spectra of **2**(BF_4^-) after adding $Zn(NO_3)_2$ (^{1}H NMR ,400 MHz, D_2O, 298 K).

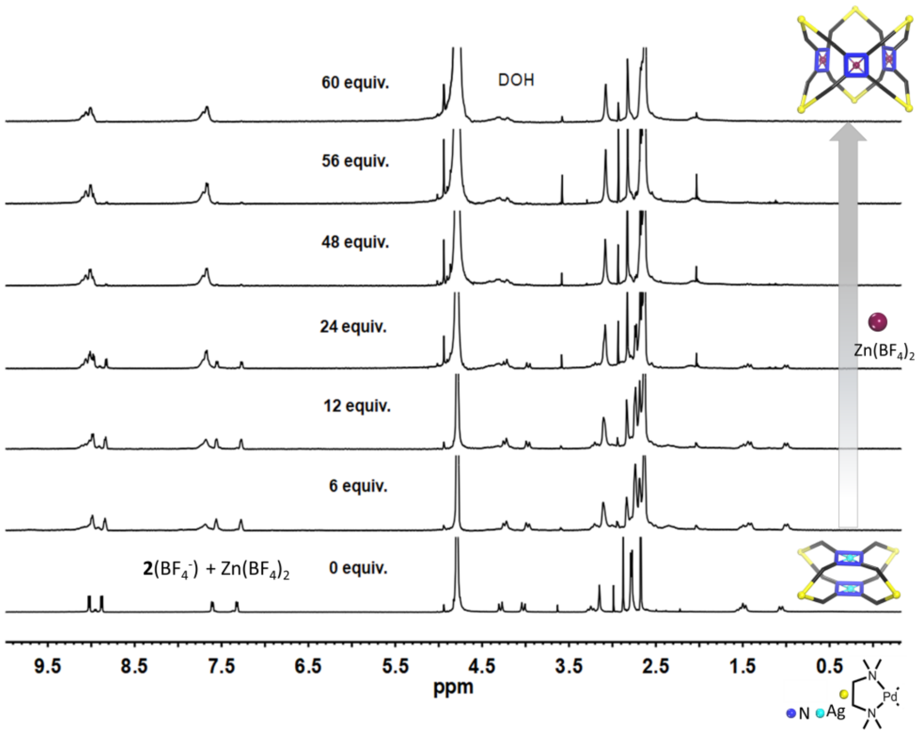

Figure S 55 The ^{1}H NMR spectra of **2**(BF_4^-) after adding $Zn(BF_4)_2$ (^{1}H NMR, 400 MHz, D_2O, 298 K).

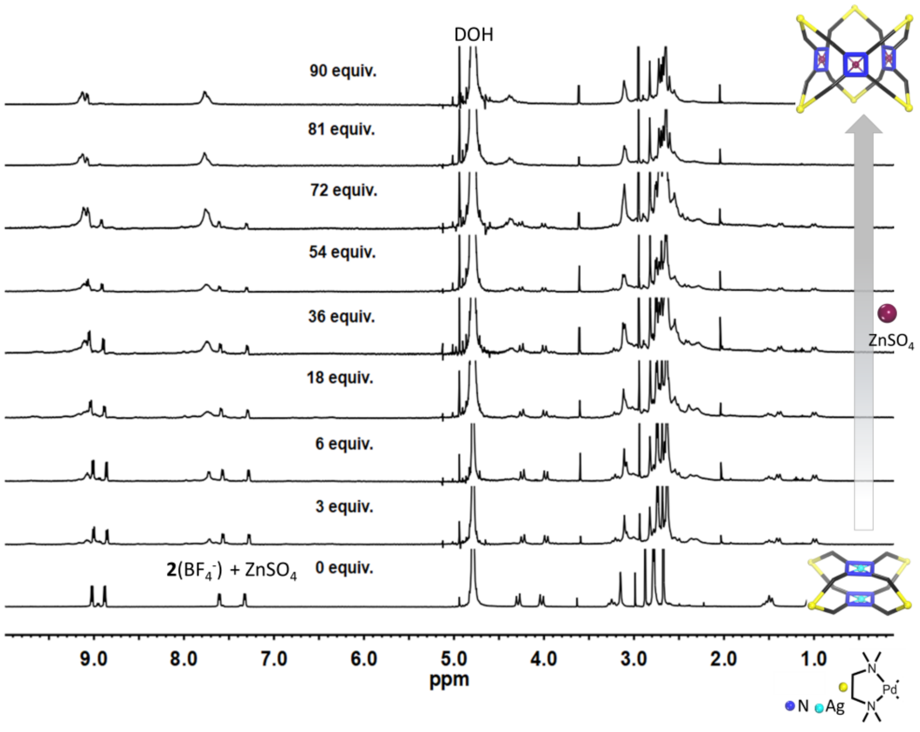

Figure S 56 The ^{1}H NMR spectra of **2**(BF_4^-) after adding $ZnSO_4$ (^{1}H NMR, 400 MHz, D_2O, 298 K).

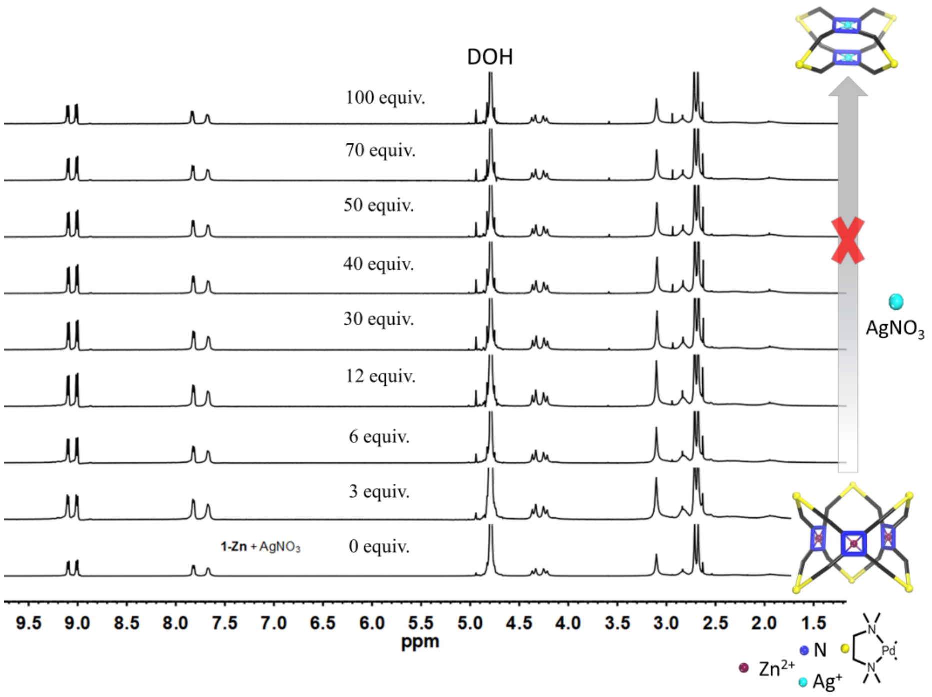

Figure S 57 The ^{1}H NMR spectra of **1-Zn** after adding AgNO$_3$ (^{1}H NMR ,400 MHz, D$_2$O, 298 K).

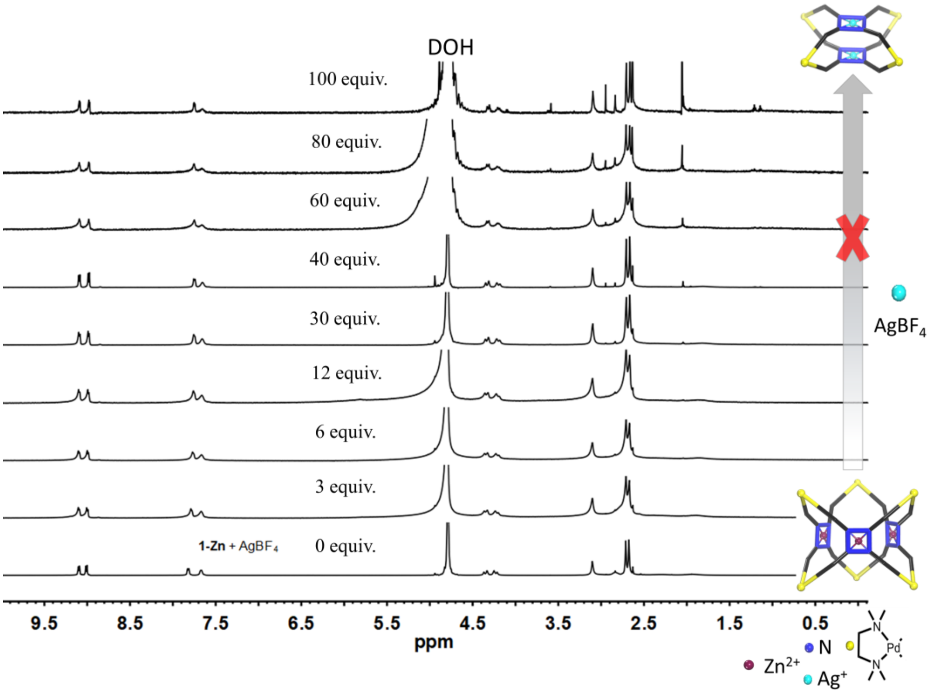

Figure S 58 The ^{1}H NMR spectra of **1-Zn** after adding AgBF$_4$ (^{1}H NMR, 400 MHz, D$_2$O, 298 K).

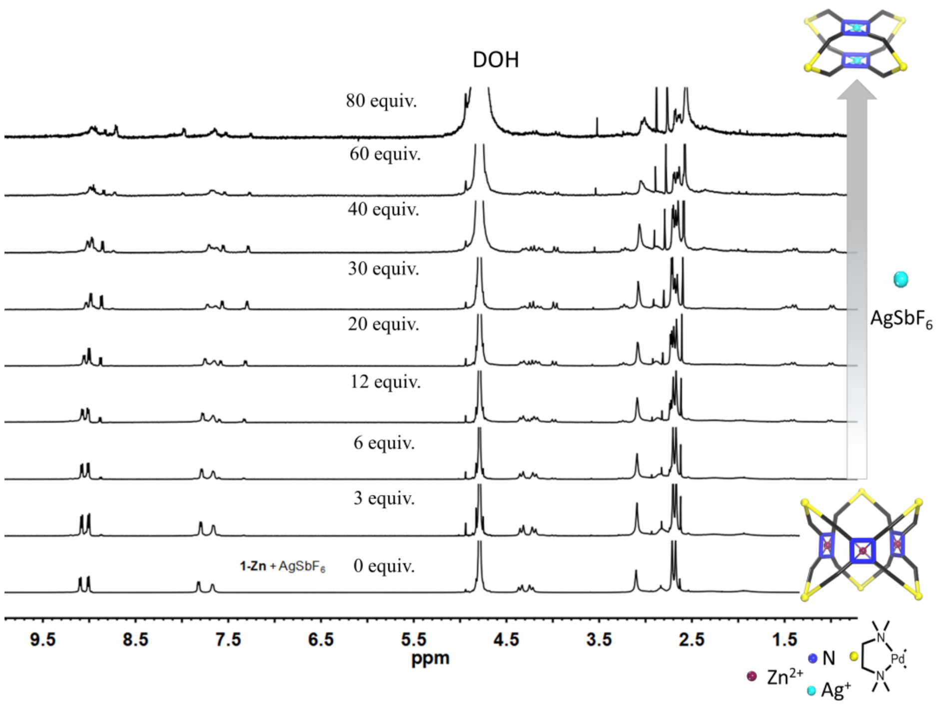

Figure S 59 The ^{1}H NMR spectra of **1-Zn** after adding $AgSbF_6$ (^{1}H NMR, 400 MHz, D_2O, 298 K).

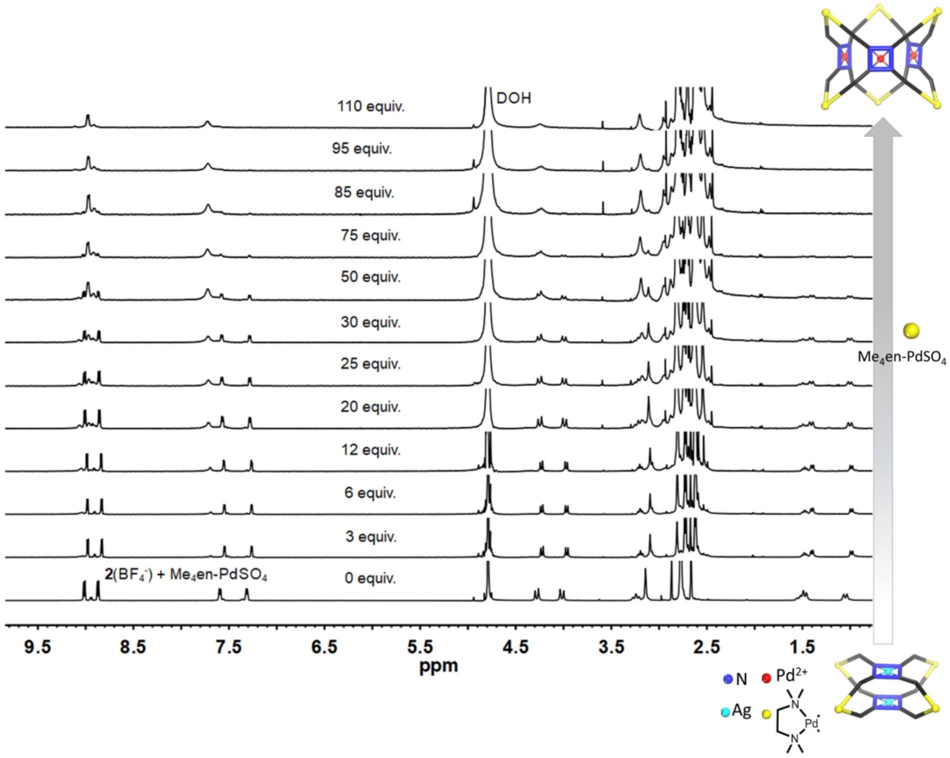

Figure S 60 The ^{1}H NMR spectra of cage **2**(BF_4^-) after adding $Me_4en\text{-}PdSO_4$ (^{1}H NMR, 400 MHz, D_2O, 298 K).

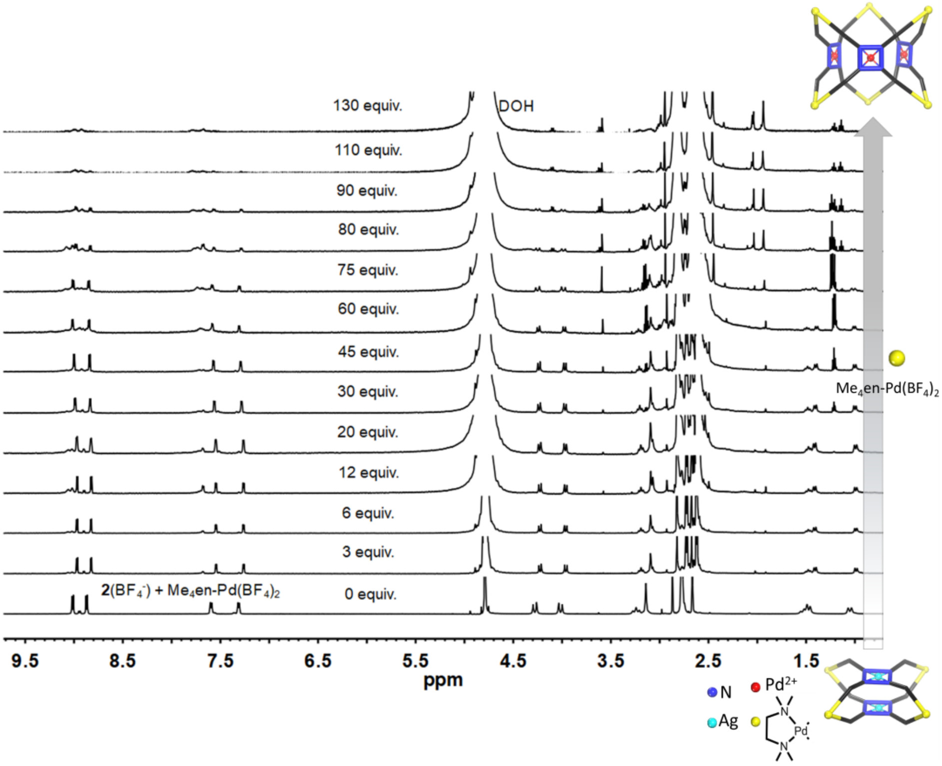

Figure S 61 The ^{1}H NMR spectra of cage **2**(BF_4^-) after adding Me$_4$en-Pd(BF_4)$_2$ (^{1}H NMR, 400 MHz, D_2O, 298 K).

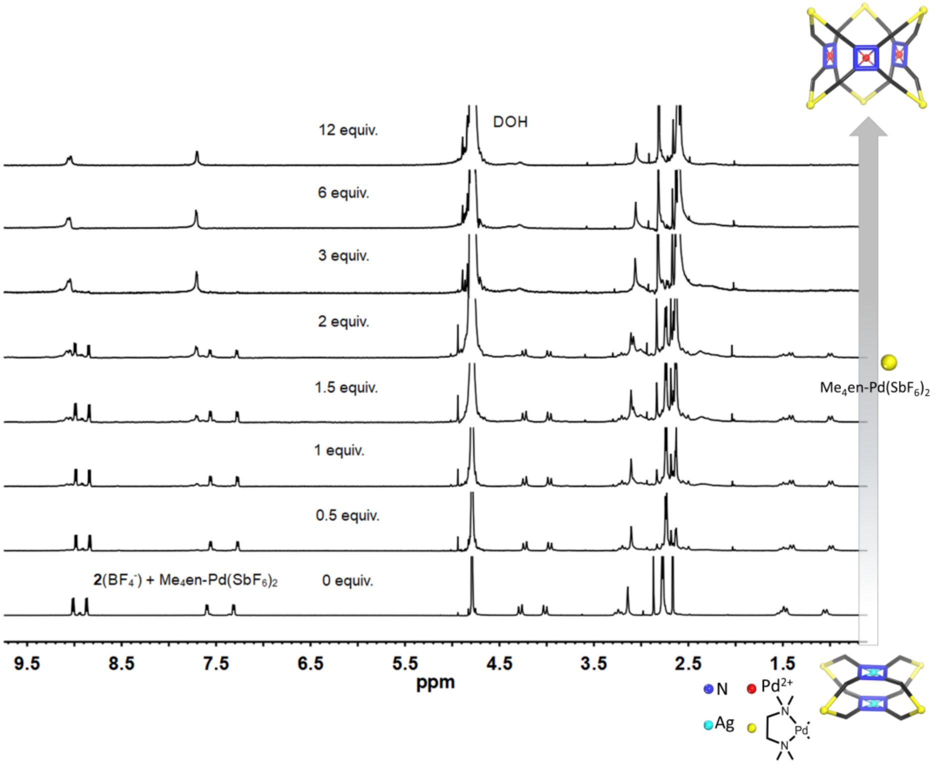

Figure S 62 The ^{1}H NMR spectra of cage **2**(BF_4^-) after adding Me$_4$en-Pd(SbF_6)$_2$ (^{1}H NMR, 400 MHz, D_2O, 298 K).

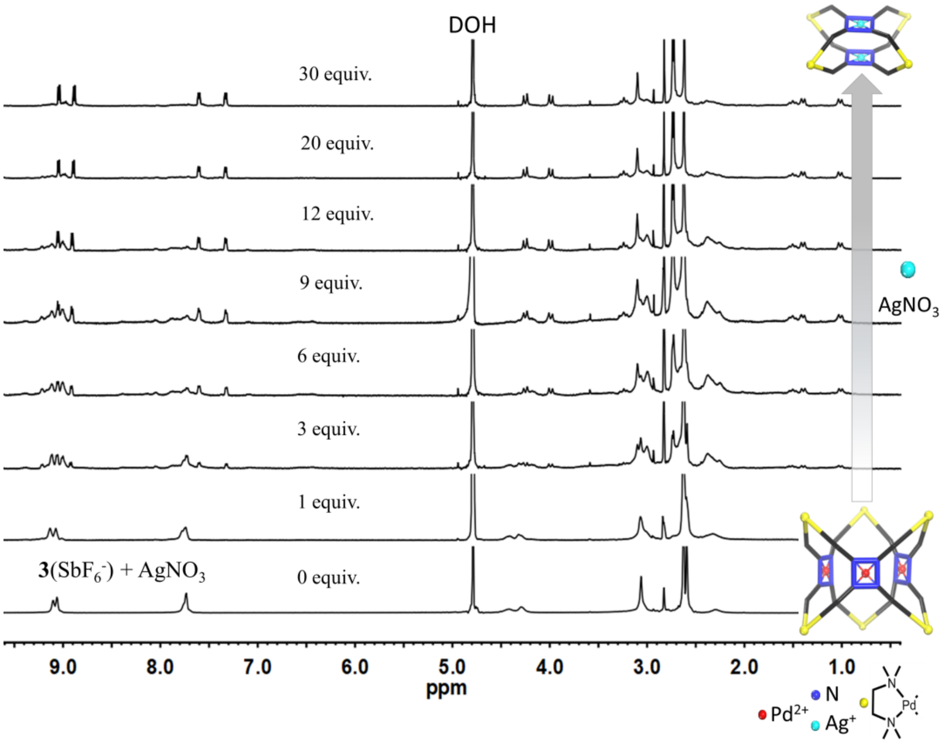

Figure S 63 The ^{1}H NMR spectra of **3**(SbF_6^-) after adding $AgNO_3$ (^{1}H NMR, 400 MHz, D_2O, 298 K).

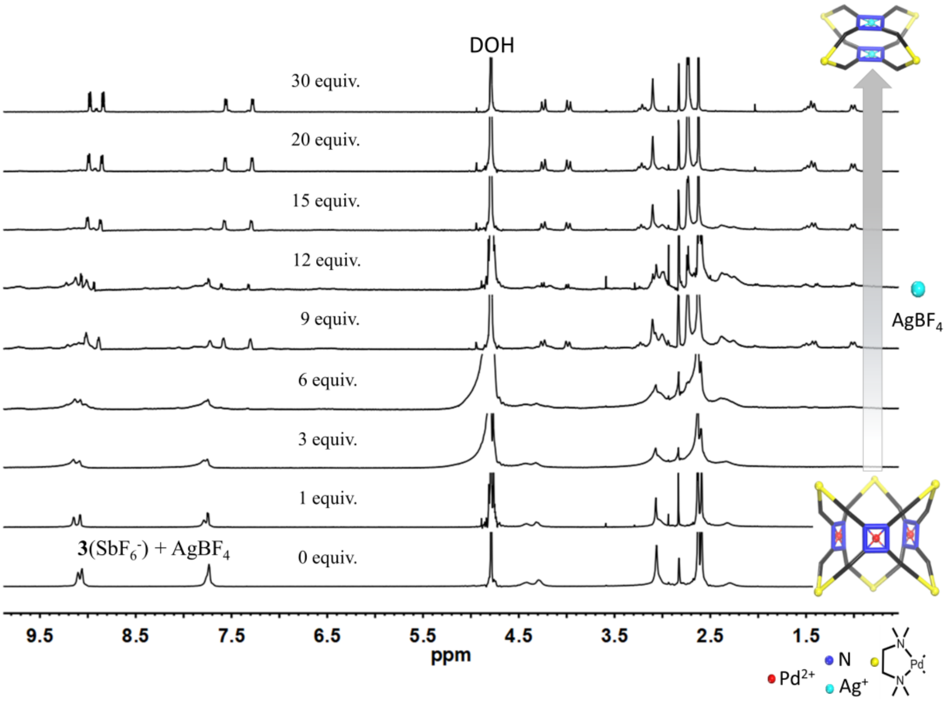

Figure S 64 The ^{1}H NMR spectra of **3**(SbF_6^-) after adding $AgBF_4$ (^{1}H NMR, 400 MHz, D_2O, 298 K).

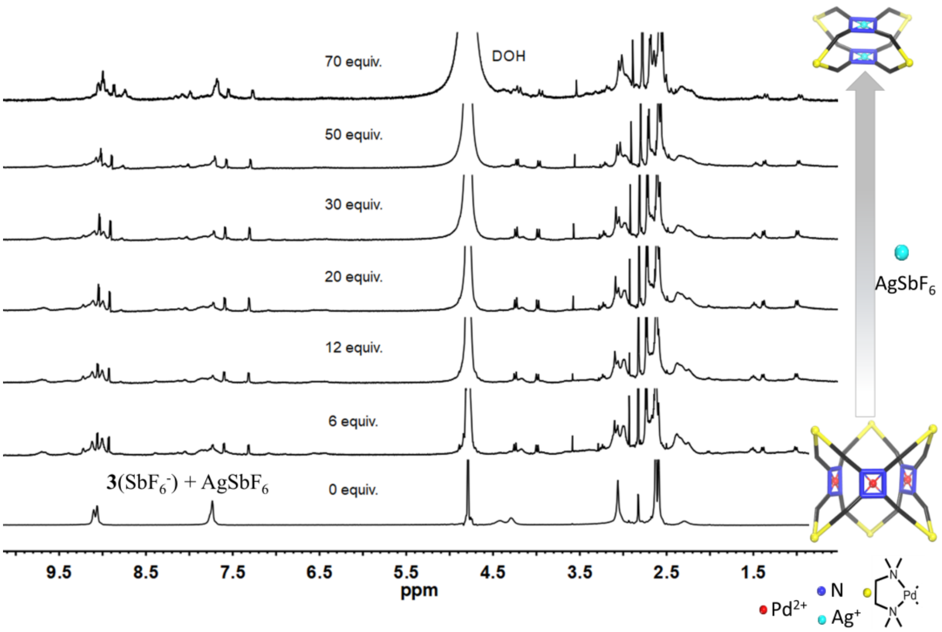

Figure S 65 The ^{1}H NMR spectra of **3**(SbF_6^-) after adding $AgSbF_6$ (^{1}H NMR, 400 MHz, D_2O, 298 K).

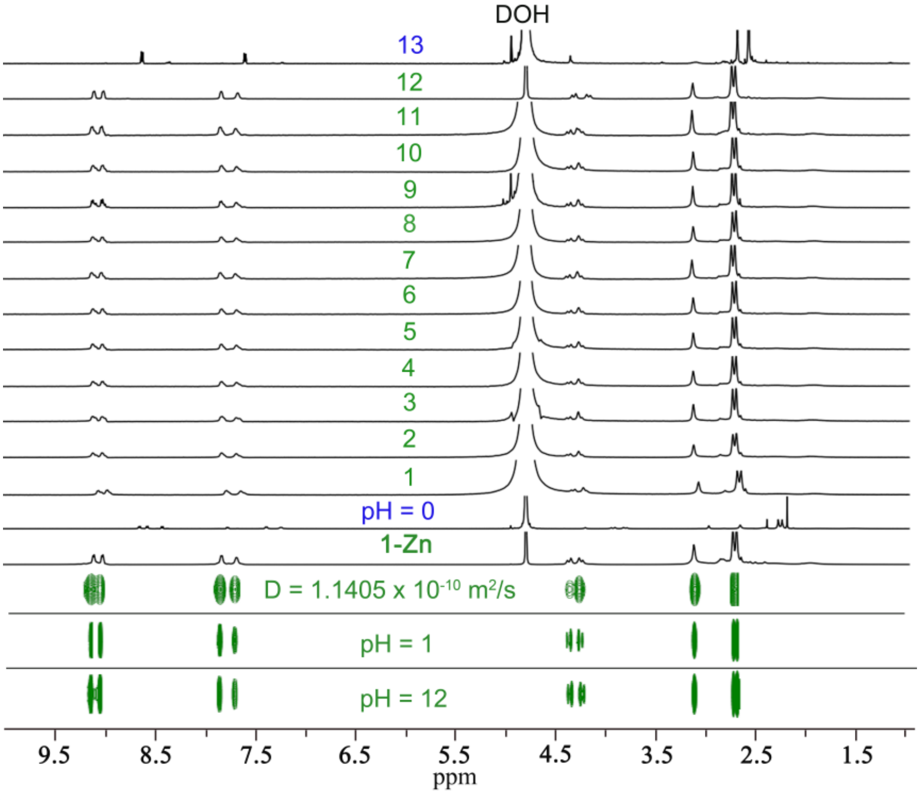

Figure S 66 The ^{1}H NMR spectra and DOSY of tube **1-Zn**(NO_3^-) under different conditions: from pH 0 to pH 13 (400 MHz, D_2O, 298 K).

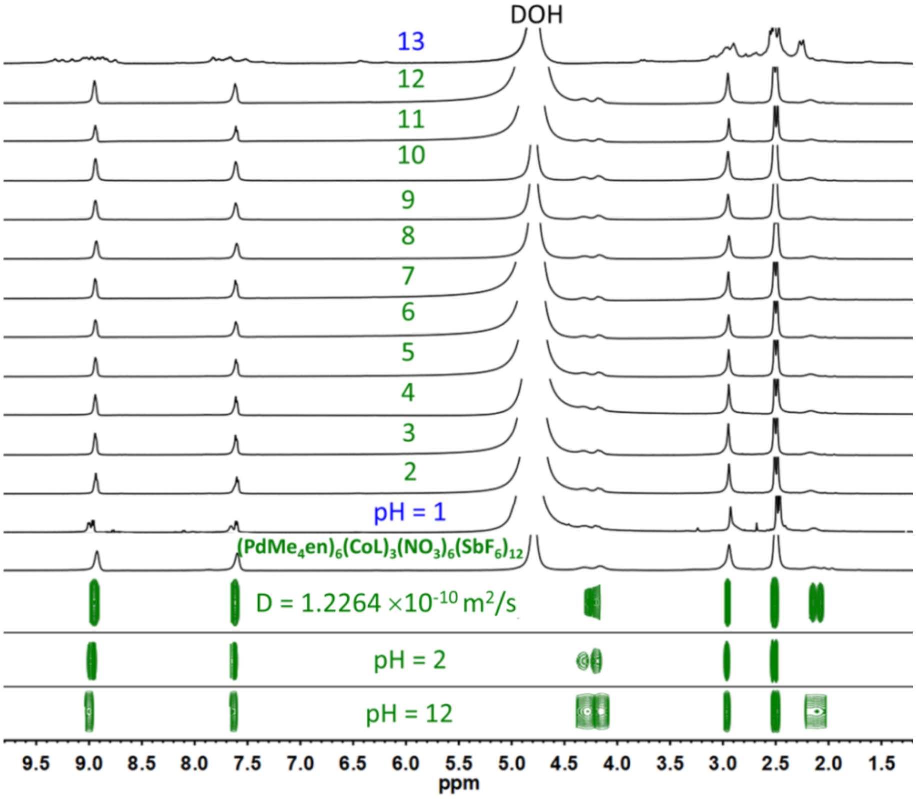

Figure S 67 The ^{1}H NMR spectra and DOSY of tube **1-Co** under different conditions: from pH 1 to pH 13 (400 MHz, D_2O, 298 K).

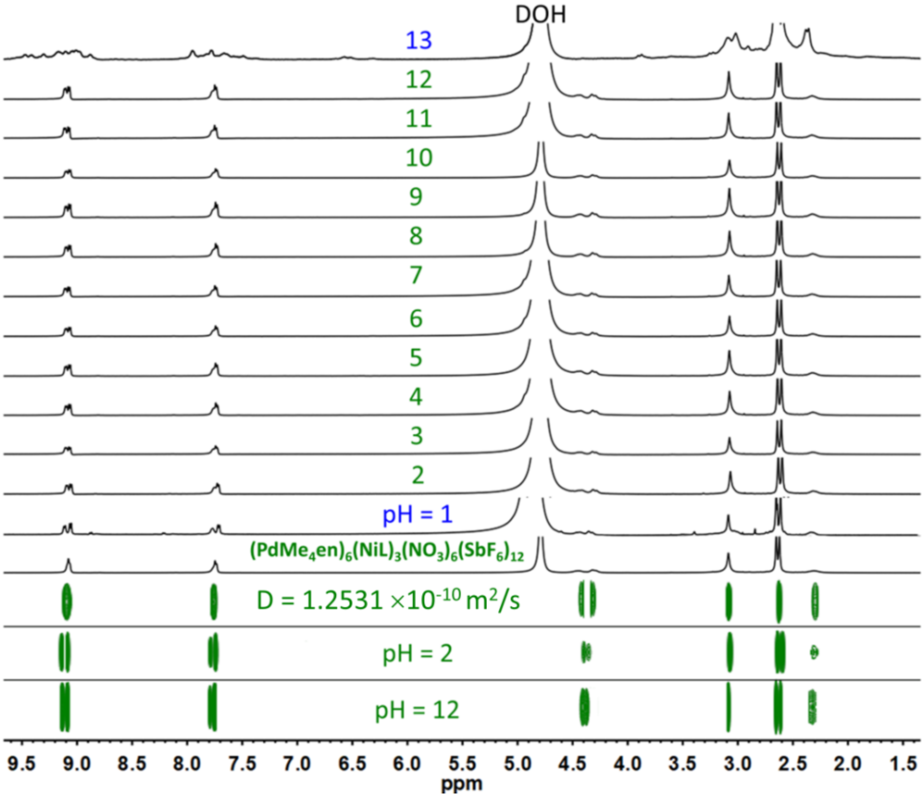

Figure S 68 The ^{1}H NMR spectra and DOSY of tube **1-Ni** under different conditions: from pH 1 to pH 13 (400 MHz, D_2O, 298 K).

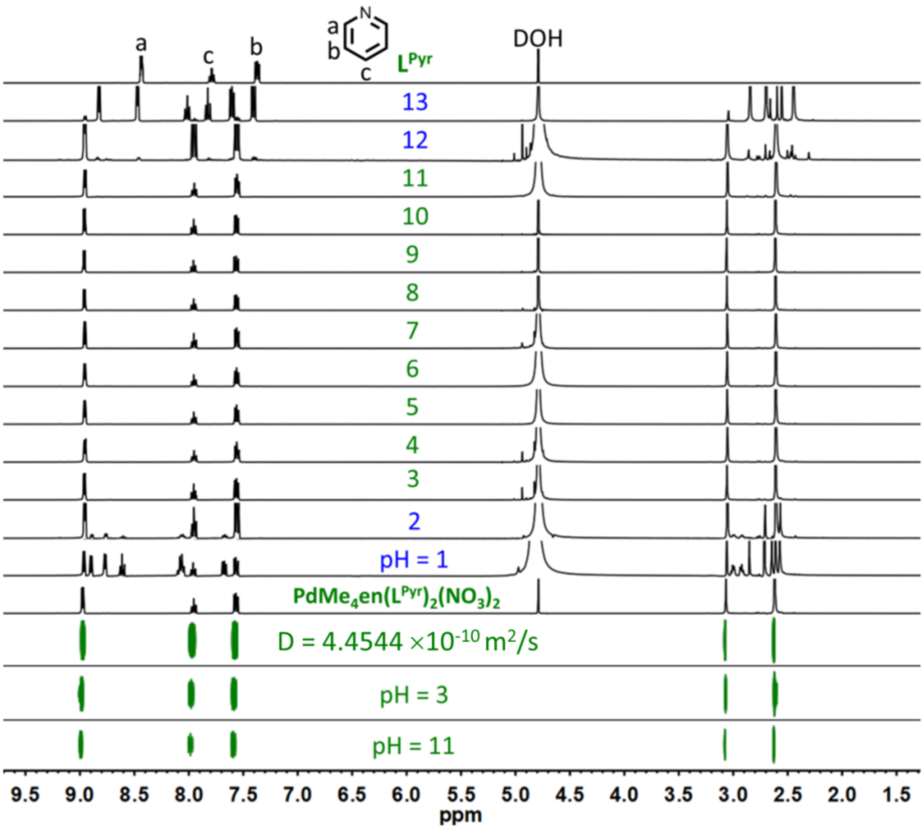

Figure S 69 The ^1H NMR spectra and DOSY of **$PdMe_4enPy_2(NO_3)_2$** under different conditions: from pH 1 to pH 13 (400 MHz, D_2O, 298 K).

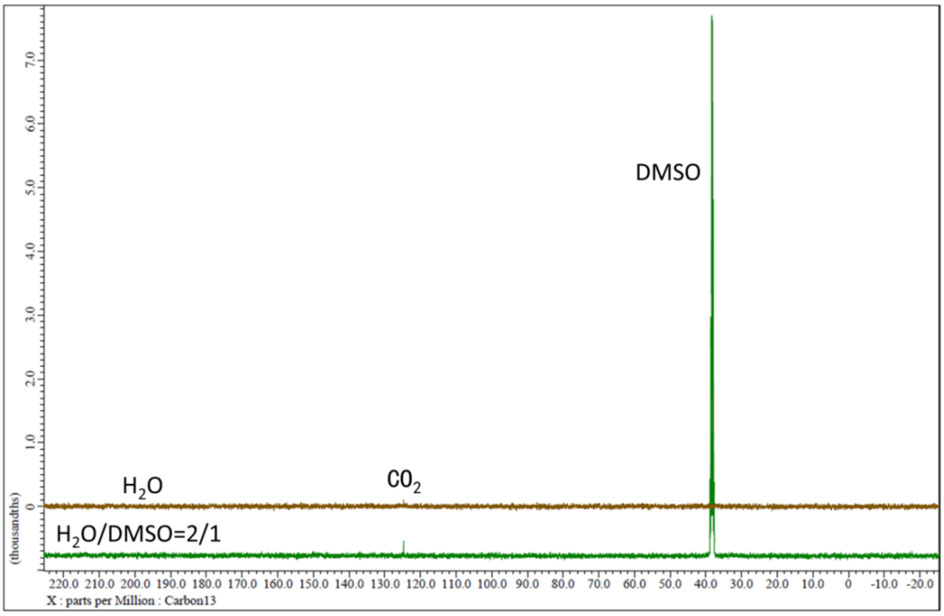

Figure S 70 The ^{13}C NMR spectra of CO_2 under different solvents. (^{13}C NMR, 101 MHz, D_2O, D_2O/DMSO-*d6*, 298 K).

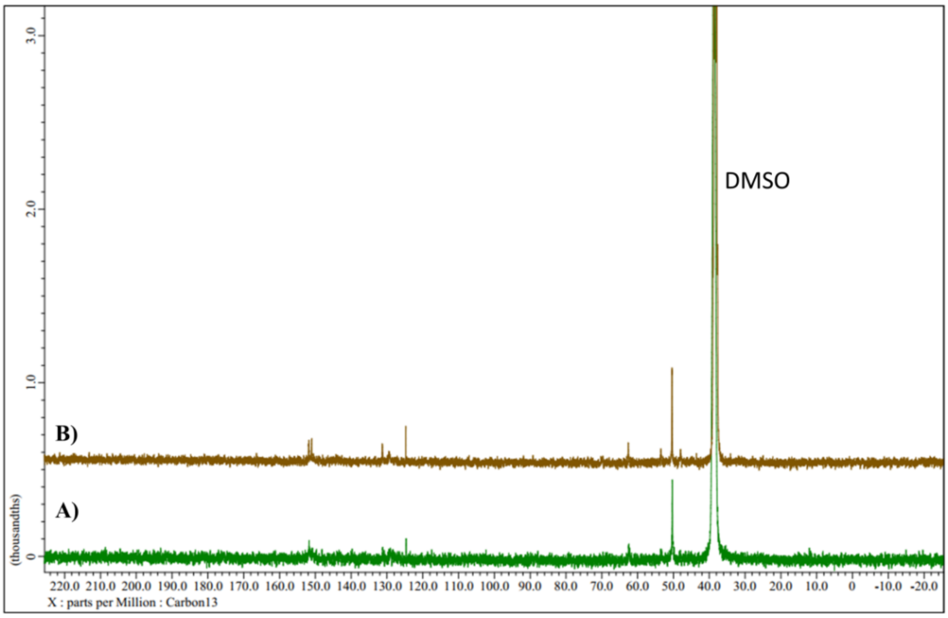

Figure S 71 The ^{13}C NMR spectra under different conditions. A) Tube **1-Co** partipicated conversion. B) Tube **1-Ni** partipicated conversion (^{13}C NMR, 101 MHz, D_2O/DMSO-$_{d6}$, 298 K).

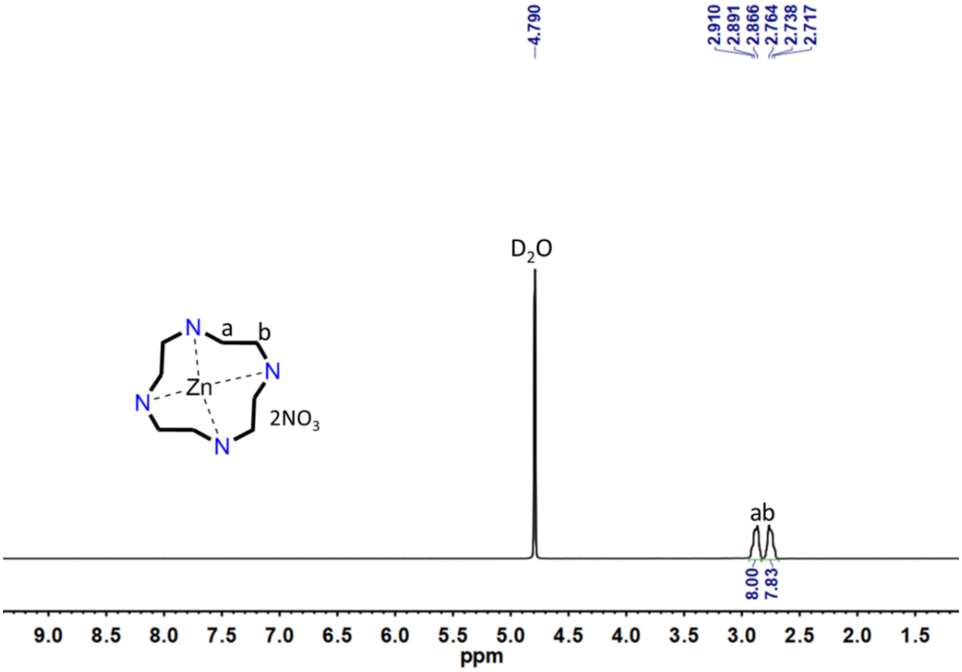

Figure S 72 The ^{1}H NMR spectrum of **[ZnL^1]**$(NO_3)_2$ (400 MHz, D_2O, 298 K).

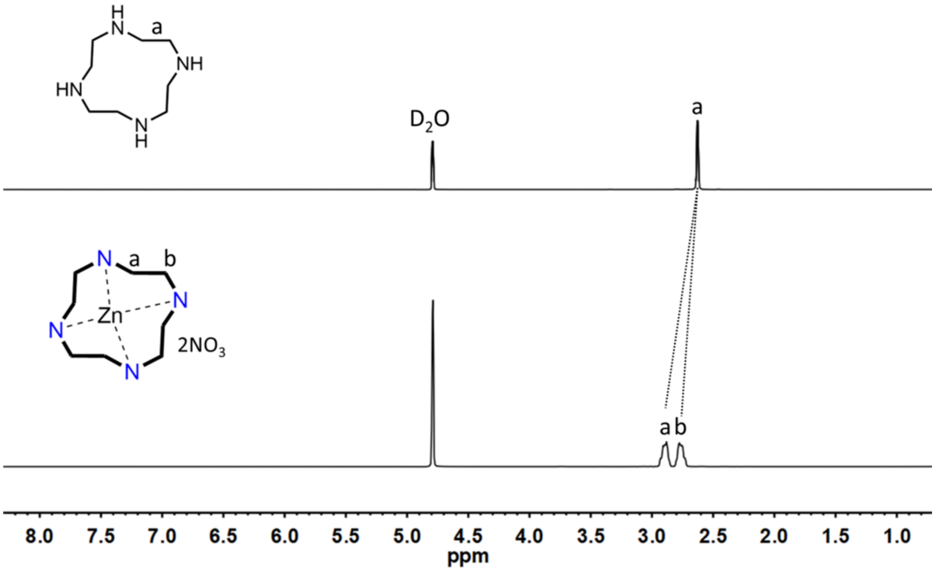

Figure S 73 The ^{1}H NMR spectra compariosn between free **L^1** and **ZnL^1**. (400 MHz, D_2O, 298 K).

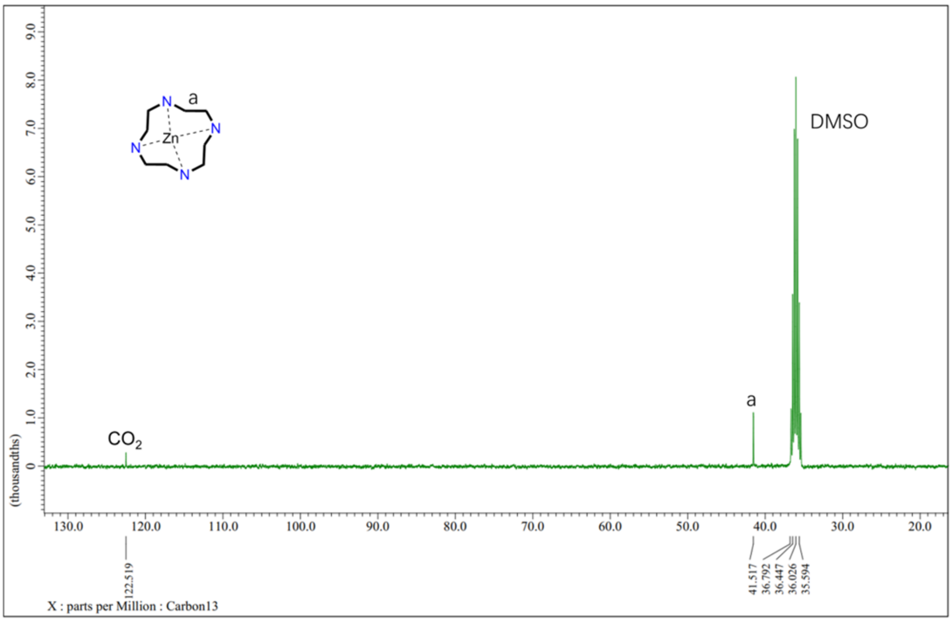

Figure S 74 The ^{13}C NMR spectrum after adding **ZnL^1**. (^{13}C NMR, 101 MHz, D_2O/DMSO-$_{d6}$, 298 K).

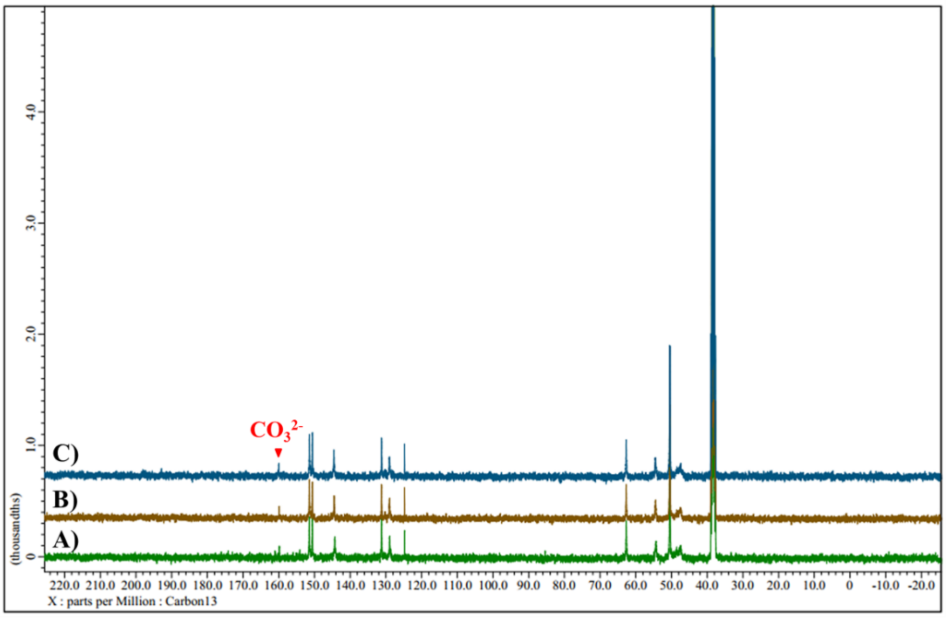

Figure S 75 The ^{13}C NMR spectra under different conditions. A) adding 0.03 mmol NaOH then stirring for 3 hours. B) Further adding 0.03 mmol NaOH then stirring for another 3 hours. C) Adding 0.03 mmol NaOH for the third then continously stirrring for 3hours. (^{13}C NMR, 101 MHz, D$_2$O/DMSO-$_{d6}$, 298 K).

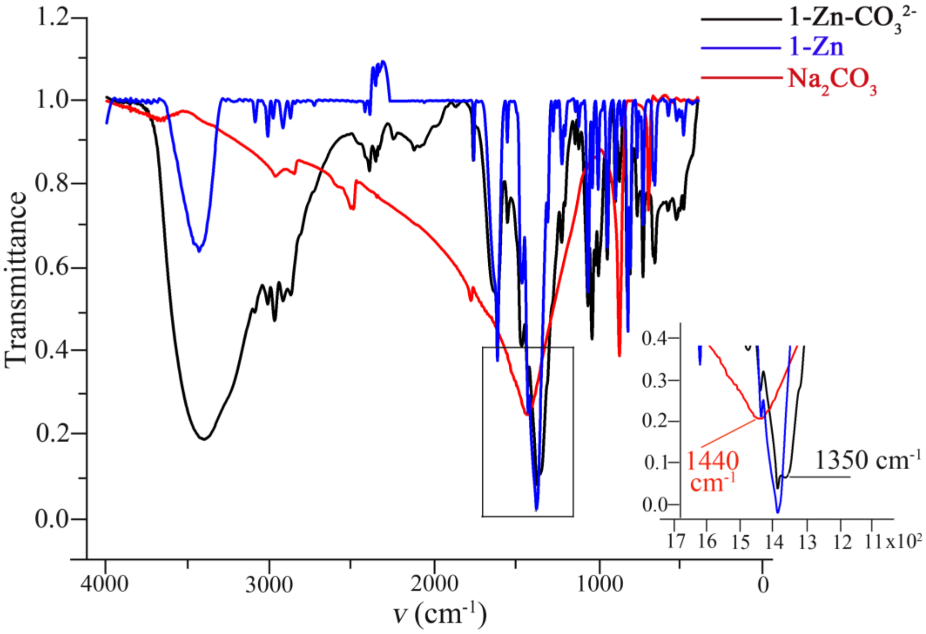

Figure S 76 The IR spectra of tube **1-Zn**, **1-Zn-CO$_3^{2-}$**, and **Na$_2$CO$_3$**.

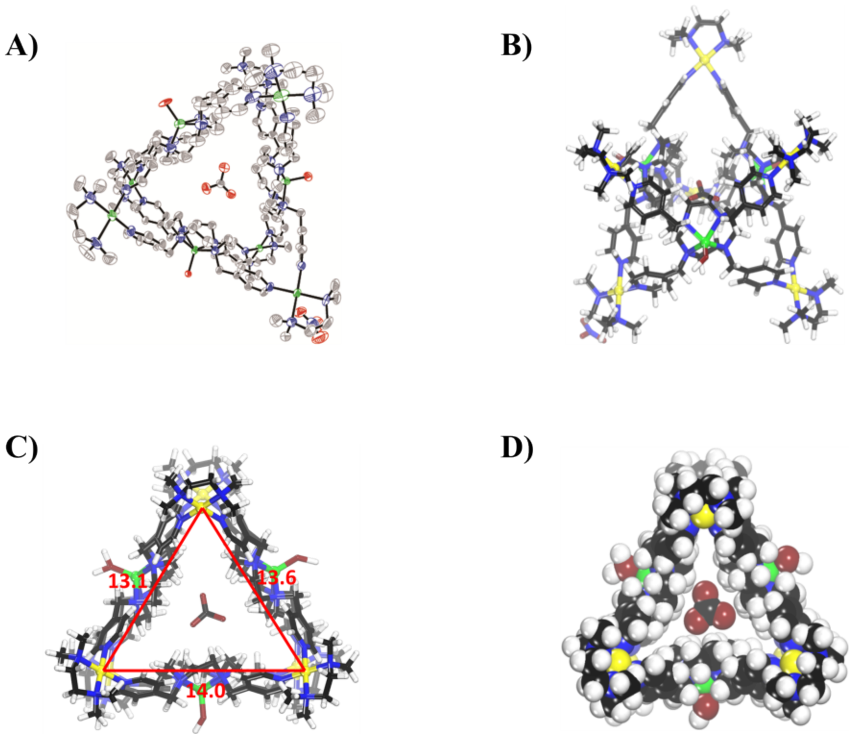

Figure S 77 The structures of tube **1-Zn-CO$_3^{2-}$**. A) Asymmetric unit. B) The crystal structure. C-D) the size of tube cavity. (black, C; blue, N; yellow, Pd; red, O; green, Zn; white, H).

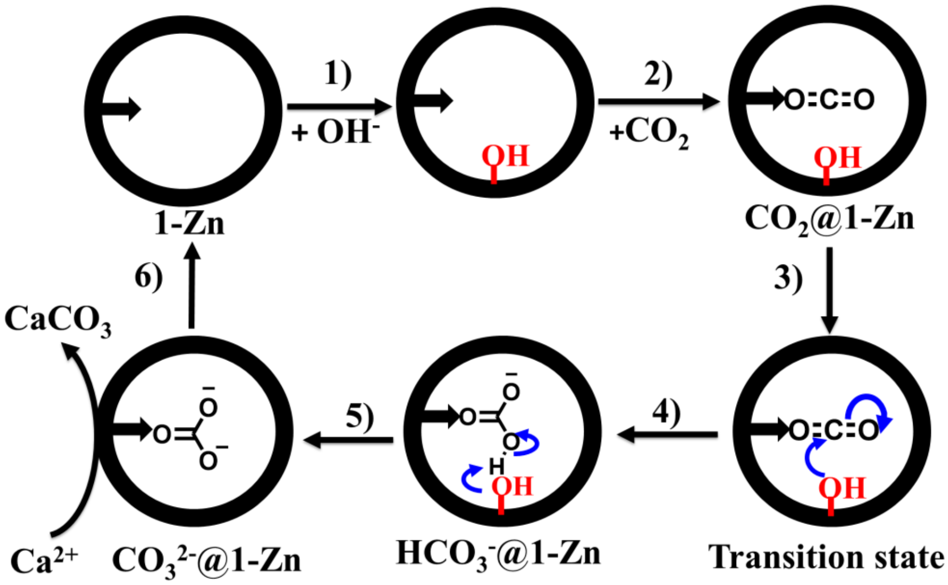

Figure S 78 A possible cavity-assisted CO$_2$ conversion process.

Table S 1 Crystal data and structure refinement for ligand **L**

Identification code	**L**
Empirical formula	$C_{33}H_{40}F_3N_8O_3S$
Formula weight	685.79
Temperature	200.01
Wavelength	0.71073 Å
Crystal system	monoclinic
Space group	$P2_1/c$
Unit cell dimensions	a = 21.6258(12) Å $\alpha = 90°$
	b = 9.9541(5) Å $\beta = 91.635(2)°$
	c = 17.1986(10) Å $\gamma = 90°$
Volume	3700.8(4) $Å^3$
Z	4
Density (calculated)	1.231 Mg/m^3
Absorption coefficient	0.145 mm^{-1}
F(000)	1444.0
Crystal size	0.10 x 0.02 x 0.02 mm^3
Theta range for data collection	4.506 to 52.852°.
Index ranges	$-27<=h<=27,-12<=k<=12,-21<=l<=18$
Reflections collected	44447
Independent reflections	7568 [$R_{int} = 0.0407$, $R_{sigma} = 0.0307$]
Completeness to theta=24.000°	99.7 %
Absorption correction	Multi-scan
Max. and min. transmission	0.7454 and 0.6903
Refinement method	Full-matrix least-squares on F^2
Data / restraints / parameters	7568 / 0 / 433
Goodness-of-fit on F^2	0.932
Final R indices [I>2sigma(I)]	$R_1 = 0.0448$, $wR_2 = 0.1223$
R indices (all data)	$R_1 = 0.0608$, $wR_2 = 0.1385$
Extinction coefficient	n/a
Largest diff. peak and hole	0.77 and -0.37 e.$Å^{-3}$
CCDC number	213475

Table S 2 Crystal data and structure refinement for **ZnL**

Identification code	**ZnL**
Empirical formula	$C_{32}H_{45}N_{10}O_9Zn$
Formula weight	779.15
Temperature	150.01
Wavelength	0.71073 Å
Crystal system	orthorhombic
Space group	Pnn2
Unit cell dimensions	a = 15.0627(9) Å α = 90°
	b = 17.4968(10) Å β = 90°
	c = 7.9686(5) Å γ = 90°
Volume	2100.1 (2) $Å^3$
Z	2
Density (calculated)	1.232 Mg/m^3
Absorption coefficient	0.642 mm^{-1}
F(000)	818.0
Crystal size	0.5 x 0.5 x 0. 2 mm^3
Theta range for data collection	5.384 to 50.054°.
Index ranges	-17<=h<=17, -20<=k<=20, -9<=l<=9
Reflections collected	44290
Independent reflections	3613 [R_{int} = 0.0311, R_{sigma} = 0.0216]
Completeness to theta=24.000°	97.4 %
Absorption correction	Multi-scan
Max. and min. transmission	0.7468 and 0.6373
Refinement method	Full-matrix least-squares on F^2
Data / restraints / parameters	3613 / 78 / 240
Goodness-of-fit on F^2	1.059
Final R indices [I>2sigma(I)]	R_1 = 0.0450, wR_2 = 0.1263
R indices (all data)	R_1 = 0.0455, wR_2 = 0.1272
Extinction coefficient	n/a
Largest diff. peak and hole	1.19 and -0.84 $e.Å^{-3}$
CCDC number	213476

Table S 3 Crystal data and structure refinement for tube **1-Zn**

Identification code	**1-Zn**
Empirical formula	$C_{132}H_{222}N_{44}O_{27}Pd_6Zn_3$
Formula weight	3692.03
Temperature	150.01
Wavelength	0.71073 Å
Crystal system	triclinic
Space group	P-1
Unit cell dimensions	a = 20.945(4) Å α = 104.189(6)°
	b = 22.830(4) Å β = 94.634(7)°
	c = 29.392(5) Å γ = 113.893(6)°
Volume	12198(4) $Å^3$
Z	2
Density (calculated)	1.005 Mg/m^3
Absorption coefficient	0.773 mm^{-1}
F(000)	3808.0
Crystal size	0.05 x 0.02 x 0.02 mm^3
Theta range for data collection	4.344 to 53.12°.
Index ranges	-26<=h<=26, -28<=k<=28, -36<=l<=36
Reflections collected	325558
Independent reflections	50369 [R_{int} = 0.0549, R_{sigma} = 0.0387]
Completeness to theta=24.000°	99.0 %
Absorption correction	Multi-scan
Max. and min. transmission	0.7454 and 0.5939
Refinement method	Full-matrix least-squares on F^2
Data / restraints / parameters	50369 / 381 / 1936
Goodness-of-fit on F^2	1.024
Final R indices [I>2sigma(I)]	R_1 = 0.0643, wR_2 = 0.1872
R indices (all data)	R_1 = 0.0801, wR_2 = 0.2036
Extinction coefficient	n/a
Largest diff. peak and hole	2.27 and -1.05 e.$Å^{-3}$
CCDC number	213469

Table S 4 Crystal data and structure refinement for cage **2**(BF_4^-)

Identification code	**2**(BF_4^-)
Empirical formula	$C_{88}H_{148}Ag_2B_2F_{20}N_{24}O_2Pd_4Si_2$
Formula weight	2673.44
Temperature	150.1(2)
Wavelength	1.3405 Å
Crystal system	triclinic
Space group	P-1
Unit cell dimensions	a = 13.5019 (3) Å □ α = 72.754(2)°
	b = 14.0260 (3) Å□□□ β = 73.765(2)°
	c = 20.0093 (5) Å□□□ γ = 80.009(2)°
Volume	3457.63(15) $Å^3$
Z	1
Density (calculated)	1.284 Mg/m^3
Absorption coefficient	4.816 mm^{-1}
F(000)	1356.0
Crystal size	0.5 x 0.5 x 0.25 mm^3
Theta range for data collection	6.378 to 105.862°.
Index ranges	-16<=h<=15, -16<=k<=16, -23<=l<=23
Reflections collected	46670
Independent reflections	12164 [R_{int} = 0.0804, R_{sigma} = 0.0522]
Completeness to theta=24.000°	99.6 %
Absorption correction	Multi-scan
Max. and min. transmission	1.0000 and 0.5679
Refinement method	Full-matrix least-squares on F^2
Data / restraints / parameters	12164 / 196 / 658
Goodness-of-fit on F^2	1.062
Final R indices [I>2sigma(I)]	R_1 = 0.0800, wR_2 = 0.2111
R indices (all data)	R_1 = 0.0840, wR_2 = 0.2144
Extinction coefficient	n/a
Largest diff. peak and hole	3.40 and -2.19 $e.Å^{-3}$
CCDC number	2131470

Table S 5 Crystal data and structure refinement for cage **2**(SO_4^{2-})

Identification code	**2**(SO_4^{2-})
Empirical formula	$C_{88}H_{144}Ag_2N_{24}O_4Pd_4$
Formula weight	2243.60
Temperature	149.99
Wavelength	0.71073 Å
Crystal system	monoclinic
Space group	C2/m
Unit cell dimensions	a = 22.785(3) Å α = 90° b = 15.8669(17) Å β = 108.536(4)° c = 20.292(2) Å γ = 90°
Volume	6955.4(13) $Å^3$
Z	2
Density (calculated)	1.071 Mg/m^3
Absorption coefficient	0.824 mm^{-1}
F(000)	2300.0
Crystal size	0.05 x 0.05 x 0.01 mm^3
Theta range for data collection	6.214 to 52.742°.
Index ranges	-28<=h<=28, -19<=k<=19, -25<=l<=25
Reflections collected	40648
Independent reflections	7261 [R_{int} = 0.0474, R_{sigma} = 0.0353]
Completeness to theta=24.000°	99.0 %
Absorption correction	Multi-scan
Max. and min. transmission	0.7455 and 0.6296
Refinement method	Full-matrix least-squares on F^2
Data / restraints / parameters	7261 / 295 / 286
Goodness-of-fit on F^2	1.049
Final R indices [I>2sigma(I)]	R_1 = 0.1138, wR_2 = 0.2942
R indices (all data)	R_1 = 0.1255, wR_2 = 0.3068
Extinction coefficient	n/a
Largest diff. peak and hole	2.72 and -1.96 $e.Å^{-3}$
CCDC number	2131471

Table S 6 Crystal data and structure refinement for tube **3**(ClO_4^-)

Identification code	**3**(ClO_4^-)
Empirical formula	$C_{132}H_{216}Cl_9N_{36}O_{36}Pd_9$
Formula weight	4160.05
Temperature	100.00(12)
Wavelength	1.54184 Å
Crystal system	monoclinic
Space group	$P2_1/m$
Unit cell dimensions	a = 20.5739(4) Å α = 90°
	b = 36.0214(10) Å β = 95.6495(15)°
	c = 31.0497(5) Å γ = 90°
Volume	22899.1(8) $Å^3$
Z	4
Density (calculated)	1.207 Mg/m^3
Absorption coefficient	7.025 mm^{-1}
F(000)	8460.0
Crystal size	0.2 x 0.1 x 0.1 mm^3
Theta range for data collection	4.316 to 156.75°.
Index ranges	-26<=h<=25, -42<=k<=40, -39<=l<=33
Reflections collected	140347
Independent reflections	45168 [R_{int} = 0.1503, R_{sigma} = 0.1301]
Completeness to theta=24.000°	96.6 %
Absorption correction	Multi-scan
Max. and min. transmission	1.0000 and 0.36348
Refinement method	Full-matrix least-squares on F^2
Data / restraints / parameters	45168 / 780 / 2017
Goodness-of-fit on F^2	0.966
Final R indices [I>2sigma(I)]	R_1 = 0.1501, wR_2 = 0.3310
R indices (all data)	R_1 = 0.2116, wR_2 = 0.3623
Extinction coefficient	n/a
Largest diff. peak and hole	1.86 and -2.03 $e.Å^{-3}$
CCDC number	213486

Table S 7 Crystal data and structure refinement for tube **1-Co**

Identification code	**1-Co**
Empirical formula	$C_{132}H_{216}Co_3N_{48}O_{36}Pd_6$
Formula weight	3866.71
Temperature	149.99
Wavelength	0.71073 Å
Crystal system	triclinic
Space group	P-1
Unit cell dimensions	a = 19.6730(14) Å □ α = 101.290(2)°
	b = 19.8305(15) Å□□□ β = 91.180(2)°
	c = 37.931(3) Å□□□□ γ = 118.770(2)°
Volume	12606.3(16) Å^3
Z	2
Density (calculated)	1.019 Mg/m^3
Absorption coefficient	0.666 mm^{-1}
F(000)	3978.0
Crystal size	0.5 x 0.5 x 0.5 mm^3
Theta range for data collection	4.306 to 50.4°.
Index ranges	-23<=h<=23, -23<=k<=23, -45<=l<=45
Reflections collected	300586
Independent reflections	45076 [R_{int} = 0.0537, R_{sigma} = 0.0373]
Completeness to theta=24.000°	99.6 %
Absorption correction	Multi-scan
Max. and min. transmission	0.7452 and 0.5410
Refinement method	Full-matrix least-squares on F^2
Data / restraints / parameters	45076 / 3328 / 2050
Goodness-of-fit on F^2	1.033
Final R indices [I>2sigma(I)]	R_1 = 0.0902, wR_2 = 0.2531
R indices (all data)	R_1 = 0.1053, wR_2 = 0.2692
Extinction coefficient	n/a
Largest diff. peak and hole	2.69 and -1.49 e.Å^{-3}
CCDC number	213472

Table S 8 Crystal data and structure refinement for tube **1-Ni**

Identification code	**1-Ni**
Empirical formula	$C_{132}H_{221}N_{37}Ni_3O_{14}Pd_6S_2$
Formula weight	3429.09
Temperature	149.99
Wavelength	0.71073 Å
Crystal system	monoclinic
Space group	C2/c
Unit cell dimensions	a = 36.029(3) Å α = 90°
	b = 20.769(2) Å β = 99.726(3)°
	c = 39.086(4) Å γ = 90°
Volume	28827(5) Å^3
Z	4
Density (calculated)	0.79 Mg/m^3
Absorption coefficient	0.607 mm^{-1}
F(000)	7104.0
Crystal size	0.5 x 0.5 x 0.3 mm^3
Theta range for data collection	4.456 to 51.476°.
Index ranges	-43<=h<=43, -25<=k<=25, -47<=l<=47
Reflections collected	314296
Independent reflections	27304 [R_{int} = 0.0721, R_{sigma} = 0.0381]
Completeness to theta=24.000°	99.4 %
Absorption correction	Multi-scan
Max. and min. transmission	0.7453 and 0.5683
Refinement method	Full-matrix least-squares on F^2
Data / restraints / parameters	27304 / 246 / 890
Goodness-of-fit on F^2	1.020
Final R indices [I>2sigma(I)]	R_1 = 0.1099, wR_2 = 0.2929
R indices (all data)	R_1 = 0.1227, wR_2 = 0.3072
Extinction coefficient	n/a
Largest diff. peak and hole	2.61 and -1.47 e.Å^{-3}
CCDC number	213473

Table S 9 Crystal data and structure refinement for tube **1-Cu**

Identification code	**1-Cu**
Empirical formula	$C_{132}H_{222}Cu_3N_{46}O_{33}Pd_6$
Formula weight	3810.56
Temperature	150.0
Wavelength	0.71073 Å
Crystal system	triclinic
Space group	P-1
Unit cell dimensions	a = 20.956(4) Å □ α = 104.463(6)°
	b = 22.765(4) Å□□□ β = 94.544(6)°
	c = 29.216(5) Å□□□□γ = 114.566(6)°
Volume	12007(3) Å^3
Z	2
Density (calculated)	1.054 Mg/m^3
Absorption coefficient	0.755 mm^{-1}
F(000)	3926.0
Crystal size	0.1 x 0.02 x 0.02 mm^3
Theta range for data collection	4.37 to 64.184°.
Index ranges	-31<=h<=31, -33<=k<=33, -43<=l<=43
Reflections collected	463000
Independent reflections	83406 [R_{int} = 0.0597, R_{sigma} = 0.0444]
Completeness to theta=24.000°	99.3 %
Absorption correction	Multi-scan
Max. and min. transmission	0.7463 and 0.6213
Refinement method	Full-matrix least-squares on F^2
Data / restraints / parameters	83406 / 2894 / 2008
Goodness-of-fit on F^2	1.060
Final R indices [I>2sigma(I)]	R_1 = 0.0665, wR_2 = 0.1968
R indices (all data)	R_1 = 0.0810, wR_2 = 0.2091
Extinction coefficient	n/a
Largest diff. peak and hole	2.76 and -1.58 e.Å^{-3}
CCDC number	213485

Table S 10 Crystal data and structure refinement for tube **1-Zn-CO$_3^{2-}$**

Identification code	**1-Zn-CO$_3^{2-}$**
Empirical formula	$C_{266}H_{438}N_{74}O_{17}Pd_{12}Zn_6$
Formula weight	6613.90
Temperature	150.15
Wavelength	1.54178 Å
Crystal system	monoclinic
Space group	C2/c
Unit cell dimensions	a = 30.2845(3) Å □ α = 90°
	b = 38.5811(3) Å□□□β = 101.5470(10)°
	c = 43.7105(5) Å□□□γ = 90°
Volume	50038.1(9) Å^3
Z	4
Density (calculated)	0.878 Mg/m^3
Absorption coefficient	4.015 mm^{-1}
F(000)	13680.0
Crystal size	0.5 x 0.4 x 0.3 mm^3
Theta range for data collection	3.756 to 153.774°.
Index ranges	-38<=h<=33, -48<=k<=47, -50<=l<=55
Reflections collected	170406
Independent reflections	50278 [R_{int} = 0.0483, R_{sigma} = 0.0366]
Completeness to theta=24.000°	98.9 %
Absorption correction	Multi-scan
Max. and min. transmission	0.7463 and 0.6213
Refinement method	Full-matrix least-squares on F^2
Data / restraints / parameters	50278 / 708 / 1706
Goodness-of-fit on F^2	1.396
Final R indices [I>2sigma(I)]	R_1 = 0.1033, wR_2 = 0.3221
R indices (all data)	R_1 = 0.1169, wR_2 = 0.3397
Extinction coefficient	n/a
Largest diff. peak and hole	2.12 and -1.23 e.Å^{-3}
CCDC number	213474

References

[1] T. H. Noh, S. M. Kim, K. H. Park, Jung O. S. Jung, *Tran. Met. Chem.* **2012**, 37, 535-540.

[2] F. Proutiere, E. Lyngvi, M. Aufiero, I. A. Sanhueza, F. Schoenebeck, *Organometallic.* **2014**, 33, 6879-6884.

[3] J. J. Wilson, E. R. Birnbaum, E. R. Batista, R. L. Martin, K. D. John, *Inorg. Chem.* **2015**, 54, 97-109.

[4] O. V. Dolomanov, L. J. Bourhis, R. J. Gildea, J. A. K. Howard, H. Puschmann, *J. Appl. Cryst.* **2009**, 42, 339-341.

[5]A. L. Spek, *J. Appl. Cryst*. **2002**, 3, 7-13.

[6] N. R.Voss, M. Gerstain, *Nucleic. Acid. Res.* **2010**, 38, W555-W562.

[7] E. F. Pettersen, T. D. Goddard, C. C. Huang, G. S. Couch, D. M. Greenblatt, E. C. Meng, T. E. Ferrin, *J. Comput. Chem.* **2004**, 13, 1605-1612.

[8] J. P. Perdew, K. Burke, M. Ernzerhof, *Phys. Rev. Lett.* **1996**,77, 3865-3868.

[9] B. Delley, *J. Chem. Phys.* **1990**, 92, 508-517.

[10] S. Grimme, *J. Comput. Chem.* **2006**, 27, 1787-1799.

[11] B. Delley, *Phys. Rev. B*. **2002**, 66, 155125-155133.

[12]Density Functional Theory Electronic Structure Program. Copyright (c) **2013**, Accelrys Inc. All rights reserved. Cite work using this program as: (a) B. Delley, *J. Chem. Phys.* **1990**, 92, 508-517; (b) B. Delley, *J. Chem. Phys.* **2000**, 113, 7756-7764. DMol^3 is available as part of Materials Studio.